



Universiteit
Leiden
The Netherlands

Hominin homelands of East Java: revised stratigraphy and landscape reconstructions for Plio-Pleistocene Trinil

Berghuis, H.W.K.; Veldkamp, A.; Adhityatama, S.; Hilgen, S.L.; Sutisna, I.; Bariato, D.H.; ... ; Joordens, J.C.A.

Citation

Veldkamp, A., Adhityatama, S., Hilgen, S. L., Sutisna, I., Bariato, D. H., Pop, E. A. L., ... Joordens, J. C. A. (2021). Hominin homelands of East Java: revised stratigraphy and landscape reconstructions for Plio-Pleistocene Trinil. *Quaternary Science Reviews*, 260. doi:10.1016/j.quascirev.2021.106912

Version: Publisher's Version

License: [Creative Commons CC BY 4.0 license](https://creativecommons.org/licenses/by/4.0/)

Downloaded from: <https://hdl.handle.net/1887/3264207>

Note: To cite this publication please use the final published version (if applicable).



Hominin homelands of East Java: Revised stratigraphy and landscape reconstructions for Plio-Pleistocene Trinil

H.W.K. Berghuis^{a, b, c, *}, A. Veldkamp^d, Shinatria Adhityatama^e, Sander L. Hilgen^{b, f}, Indra Sutisna^g, Didit Hadi Barianto^h, Eduard A.L. Pop^{a, b}, Tony Reimann^{i, n}, Dida Yurnaldi^j, Dian Rahayu Ekowati^e, Hubert B. Vonhof^k, Thijs van Kolfschoten^{a, l}, Truman Simanjuntak^e, J.M. Schoorlⁱ, Josephine C.A. Joordens^{a, b, f, m}

^a Faculty of Archaeology, Leiden University, P.O. Box 9514, Leiden, the Netherlands

^b Naturalis Biodiversity Center, P.O. Box 9517, Leiden, the Netherlands

^c Sealand Coastal Consultancy, van Baerlestraat 140, Amsterdam, the Netherlands

^d Faculty ITC, University of Twente, P.O. Box 217, 7500 AE, Enschede, the Netherlands

^e Pusat Penelitian Arkeologi Nasional (PUSLIT ARKENAS), Indonesia, Jl. Condet Pejaten No.4, Jakarta, 12510, Indonesia

^f Faculty of Science, Vrije Universiteit, de Boelelaan 1085, 1081HV, Amsterdam, the Netherlands

^g Geological Museum, Jl. Diponegoro 57, Bandung, Jawa Barat, 40122, Bandung, Indonesia

^h Department Geological Engineering, Universitas Gadjah Mada, Jl. Bulaksumur, Yogyakarta, Daerah Istimewa, Yogyakarta, 55281, Indonesia

ⁱ Soil Geography and Landscape Group & Netherlands Centre for Luminescence Dating, Wageningen University, P.O. Box 9101, 6700 HB, Wageningen, the Netherlands

^j Center for Geological Survey of Indonesia, Jl. Diponegoro 57, Bandung, Jawa Barat, 40122, Bandung, Indonesia

^k Max Planck Institute for Chemistry, Hahn-Meitner-Weg 1, 55128, Mainz, Germany

^l Institute of Cultural Heritage, Shandong University, 72 Binhai Highway, Qingdao, 266237, China

^m Faculty of Science and Engineering, Maastricht University, Kapoenstraat 2, 6211KW, Maastricht, the Netherlands

ⁿ Geomorphology & Geochronology Group, Institute for Geography, University of Cologne, Albertus-Magnus-Platz, 50923, Köln, Germany Ningen, the Netherlands

ARTICLE INFO

Article history:

Received 24 December 2020

Received in revised form

17 February 2021

Accepted 18 March 2021

Available online 16 April 2021

Handling Editor: Danielle Schreve

Keywords:

Pleistocene

Stratigraphy

Sedimentology

Homo erectus

Vertebrate palaeontology

Volcanism

Sea-level changes

Climate change

Solo River

Sundaland

ABSTRACT

Trinil (Java, Indonesia) yielded the type fossils of *Homo erectus* and the world's oldest hominin-made engraving. As such, the site is of iconic relevance for paleoanthropology. However, our understanding of its larger geological context is unsatisfactory. Previous sedimentological studies are around 100 years old and their interpretations sometimes contradictory. Moreover, the existing stratigraphic framework is based on regional correlations, which obscure differences in local depositional dynamics. Therefore, a new and more local framework is urgently needed. We carried out a comprehensive geological study of the Trinil area. Using a Digital Elevation Model, we identified seven fluvial terraces. Terrace deposits were described and OSL-dated and fluvial behaviour was reconstructed. The terraces were correlated with terraces of the Kendeng Hills (e.g. the hominin-bearing Ngandong terrace) and date back to the past ~350 ka. Thus far, most of the Trinil terraces and their deposits had remained unidentified, confounding sedimentological and stratigraphic interpretations. The exposed pre-terrace series has a thickness of ~230 m. Together with the terraces, it forms a ~3 Ma record of tectonism, volcanism, climate change and sea-level fluctuations. We subdivided the series into five new and/or revised stratigraphic units, representing different depositional environments: Kalibeng Formation, Padas Malang Formation, Batu Gajah Formation, Trinil Formation and Solo Formation. Special attention was paid to erosional contacts and weathering profiles, forming hiatuses in the depositional series, and offering insight into paleoclimate and base-level change. The Trinil Formation provides a new landscape context of *Homo erectus*. Between ~550 and 350 ka, the area was part of a lake basin (Ngawi Lake Basin), separated from the marine base level by a volcanic barrier, under dry, seasonal conditions and a regular supply of volcanic ash. An expanding and retreating lake provided favourable living conditions for hominin populations. After 350 ka, this role was taken over by the perennial Solo River. Landscape reconstructions suggest that the Solo formed by headward erosion and stream piracy, re-connecting the Ngawi Lake Basin to the plains in the

* Corresponding author. Faculty of Archaeology, Leiden University, P.O. Box 9514, Leiden, the Netherlands.

E-mail address: harold.berghuis@naturalis.nl (H.W.K. Berghuis).

west. Our study offers a local framework, but its Pleistocene landscape record has regional significance. Most of all, it forms a much-needed basis for future, detailed studies on the build-up of the hominin site of Trinil, its fossil assemblages and numerical ages.

© 2021 The Author(s). Published by Elsevier Ltd. This is an open access article under the CC BY license (<http://creativecommons.org/licenses/by/4.0/>).

1. Introduction

Trinil (East Java, Indonesia, Fig. 1) is the discovery site of the world’s first deliberately sought fossils of a transitional form between apes and humans (Dubois, 1894a). Originally named *Pithecanthropus erectus*, these specimens are now regarded as the type fossils of *Homo erectus* (Mayr, 1950). The site yielded thousands of vertebrate fossils (Dubois, 1907; Selenka and Blanckenhorn, 1911) that play a key role in regional Pleistocene vertebrate biostratigraphy (Von Koenigswald, 1934, 1935; De Vos, 1982; Sondaar, 1984) and biogeography (Van den Bergh et al., 1996; Van der Geer, 2019). Moreover, a recently discovered fossil freshwater shell from Trinil, carved with a geometric pattern, is regarded as the world’s oldest hominin-made engraving (Joordens et al., 2015).

Despite the importance of Trinil for faunal (including hominin) evolution, our understanding of the local geology is still based on over 100 years old sedimentological studies, often with contradictory interpretations (e.g. Dubois, 1908; Carthaus, 1911). Moreover, Duyfjes (1936, 1938) introduced a regional stratigraphy that is still

in use today (e.g. Zaim, 2010; Joordens et al., 2015; Puspaningrum et al., 2020). However, this framework does not take into account the dynamic development of emerging Java, under the influence of volcanism, tectonism and sea-level fluctuations, with great differences in depositional environments across relatively short distances. Duyfjes’ regional stratigraphic units are partly based on correlations between outcrops, combining strata with different facies in one unit, which deprives us of a detailed insight into local depositional processes and ages. This unsatisfactory state of the art hampers understanding of the geology in the Trinil area and confirms that a local approach is urgently needed. Our study aims to establish a comprehensive sedimentological, stratigraphic and geochronological framework for the sediments exposed in Trinil and surroundings. We use detailed field observations and modern facies models to reconstruct depositional settings and landscapes. Our study does not include a detailed re-inventory of Dubois’ excavation site. This will be addressed in a separate paper (Hilgen et al. in prep.).

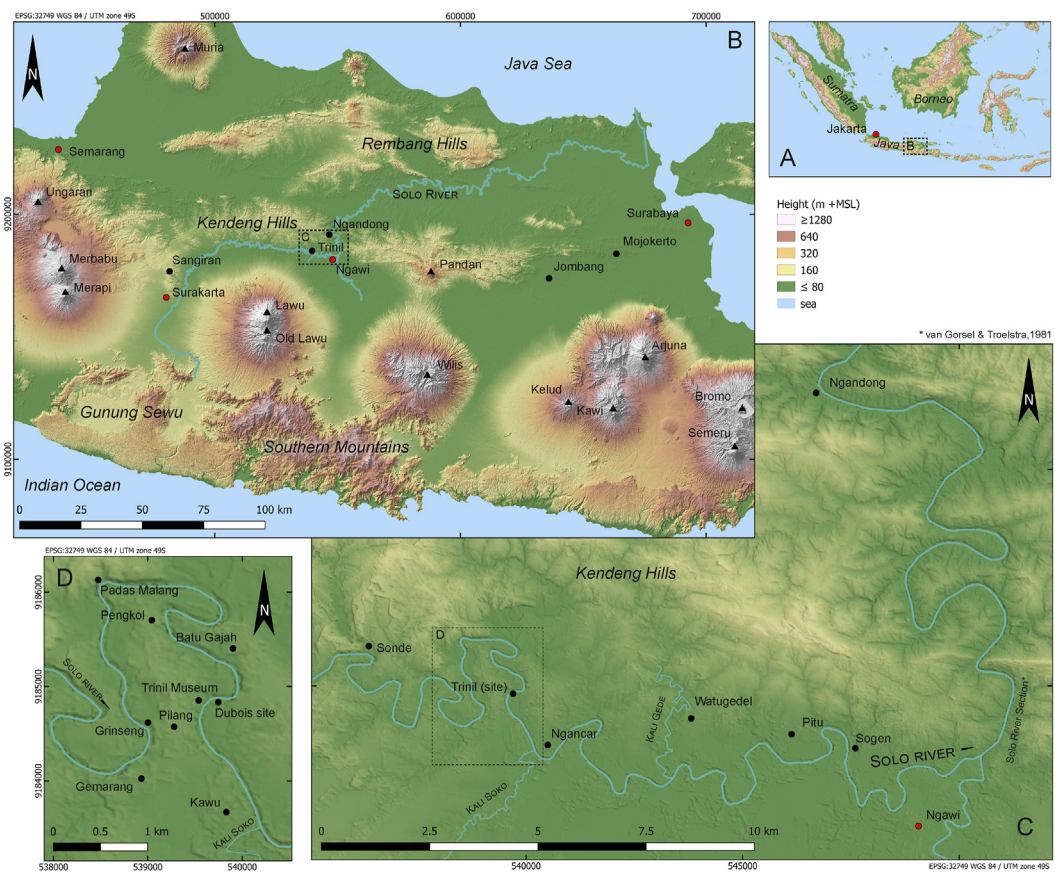


Fig. 1. (A) The Indonesian archipelago with the larger study area on the eastern part of Java, (B) Physiography of Central and East Java and sites mentioned in the text, (C) The study area between Sonde and Ngawi, (D) The Solo River meander of Trinil, Map data: GTOPO30 (A), ALOS (B), TanDEM-X © DLR 2019 (C and D).

2. Background

2.1. Setting, volcanism and tectonism

The Trinil area forms an inland plain, ca. 60 m above sea level, bounded in the north by the Kendeng Hills and in the south by the volcano Lawu (Fig. 1C). The Solo River lies entrenched in a ca. 15 m deep channel, exposing a sedimentary series dominated by Pleistocene volcanoclastics. East of Trinil, the Solo changes course to the north and crosses the Kendeng Hills. Here the riverbanks expose folded Tertiary marine strata.

In the Miocene, most of eastern Java was part of a marine retroarc basin located north of an east-west trending volcanic arc (Lunt, 2013). In the Late Miocene, volcanism ceased and the basin became subject to compression and uplift (Hamilton et al., 1979; Smyth et al., 2008). By the end of the Pliocene, east-west directed thrust and fold zones developed and emerged from the sea: the Rembang and Kendeng Hills and the Southern Mountains (Satyana et al., 2004; Clements et al., 2009). Between these ridges shallow marine zones prevailed, most of which gradually emerged later in the Pleistocene.

In the Early Pleistocene, volcanism returned, mainly building up stratovolcanoes in the low-lying zone between the Southern Mountains and the Kendeng Hills (van Bemmelen, 1949; Soeria-Atmadja et al., 1994). The Wilis was among the first eruption centers. Its core rocks date to 1.9–1.8 Ma (Hartono, 1994). Lawu is a young volcano, but along its southern flanks are the remains of a cone known as Old Lawu. Its core rocks were never dated, but its slopes have a dissected morphology similar to Wilis (Fig. 1), suggesting a similar age.

2.2. Previous work on sedimentology and stratigraphy

Dubois collected fossils from tuffaceous strata that he called the Trinil Beds. He noted cross-bedding and interbeds of rounded gravel, which convinced him that the material is of fluvial origin (Dubois, 1894a, 1895, 1907). He related the volcanoclastic composition of the sediment to contemporaneous volcanic activity. Based on paleontological analyses, he assigned the tuffs to the Late Pliocene or Early Pleistocene. Volz (1907) regarded the tuffs as volcanic debris flows from the Lawu, representing a long depositional phase covering most of the Pleistocene. Elbert (1908) agreed with Dubois on a fluvial depositional background, but suggested that the tuffs form two series: the lower series constitutes the actual Trinil Beds, the higher series is significantly younger and was deposited by the Solo. Carthaus (1911) described the larger geological context around Trinil and distinguished three lithological units, from old to young: calcareous beds with molluscs, volcanic breccias, and fossiliferous tuff. He recognized the calcareous strata as coastal deposits and the overlying breccias as a terrestrial lahar. He regarded the upper boundary of the breccias as the undulating lahar surface, after its flow had ceased. He claimed that the overlying fossiliferous tuffs (Dubois' Trinil Beds) formed in ponds on the lahar surface, referring to interbedded clays with leaf imprints. For him, occasional cross-bedding represents episodes of overflowing ponds. Van Es (1931) regarded the upper boundary of the marine, mollusc-bearing unit as an unconformity, representing Early Pleistocene exposure. He agreed with Dubois' interpretation of the Trinil Beds as a fluvial deposit, but in contrast to earlier researchers, he did not regard the sediment as primary volcanic material, but as fluvially supplied erosion material, referring to interbeds of well-rounded andesite gravel.

2.3. Duyfjes' regional stratigraphy

Duyfjes (1936, 1938) developed a regional stratigraphy, based on reference sections near Jombang, ca. 100 km east of Trinil. He described marine calcareous mudstones and diatomaceous mudstones, which he assigned to the Lower and Upper Kalibeng Formations, assuming a Pliocene age. These grade upwards into marine clays, deltaic sandstones and fluvial sandstones, which he assigned to the Early Pleistocene Pucangan Formation and the Middle Pleistocene Kabuh Formation, placing the unit boundary halfway the fluvial sandstones. Duyfjes used the units to map the Kendeng Hills and adjacent areas, over a distance of more than 150 km. Moving away from his reference sections, he had difficulties tracing his units and frequently relied on extrapolations ('parallelization'). The sandy marine deltas, which form the main Pleistocene landscape element of Jombang, are absent around Trinil. Nevertheless, Duyfjes applied his stratigraphic format to the Trinil series and assigned the calcareous strata to the Lower and Upper Kalibeng Formation, the breccias to the Pucangan Formation and the fossiliferous tuffs (Dubois' Trinil Beds) to the Kabuh Formation. Following Van Es (1931), Duyfjes regarded the Kabuh Formation as a fluvial deposit made up of erosion material. Higher-up in the Trinil series, he noted primary volcanoclastic sediment, which he assigned to the Notopuro Formation.

2.4. Discovery of fluvial terraces

Ter Haar (1934) described Solo terraces in the transverse valley through the Kendeng Hills (Fig. 1C). One of these terraces, near the village of Ngandong, appeared to be rich in vertebrate fossils including *Homo erectus* (Oppenoorth, 1932). This shed new light on Elbert's (1908) earlier suggestion on the presence of Solo deposits around Trinil. Ter Haar assumed that the Trinil Beds are the equivalent of the Ngandong terrace deposits. Lehmann (1936) found that the highest part of the plains around Trinil forms flat-topped, gravelly surfaces, which he referred to as the High Terrace. He regarded this terrace as the equivalent of the fossiliferous terrace of Ngandong. He noted that the gravelly surface layer truncates the Trinil Beds and concluded that the latter forms an older, pre-Solo deposit. Lehmann also recognized a 'Low Terrace': smaller surfaces that locally border the river, standing out ca. 7 m above low water level. Duyfjes (1936) added the sediment of Lehmann's terraces to his Trinil stratigraphy as 'Terrace Deposits'.

2.5. Problems, aims and objectives

The great differences between the depositional series of Jombang and Trinil reflect different depositional landscapes with unknown (age) relations. It makes the use of Duyfjes' regional stratigraphic units in Trinil inappropriate. Duyfjes regarded his Trinil stratigraphy as an uninterrupted series, which is unlikely, as it forms a ~3 Ma record of highly dynamic coastal and terrestrial deposition. Such series generally have a complex build-up, of various depositional stages and hiatuses.

A remarkable side-effect of the introduction of Duyfjes' stratigraphic framework is that it ended the previous discussion on the depositional background of the Trinil series, as if the new unit names provided final answers to earlier disputes (e.g. Soeradi et al., 1985).

Since the 1930s there have been major advances in the analysis of fluvial and pyroclastic facies and in fluvial dynamics controlling incision and deposition, allowing us to re-evaluate the complex

geology of Trinil with a fresh view. This is an essential step, aiming for a better understanding of the context of the excavation sites and the excavated fossils.

The objectives of our field study are: 1) to develop coherent models of local depositional environments, against a background of volcanism, tectonism, sea-level fluctuations and climate change; and 2) to define new, local stratigraphic units, which follow major changes in depositional setting.

Special attention will be paid to the role of fluvial terraces and terrace-related deposits. Elbert's (1908) and Bartstra's (1982) suggestion of a more widespread occurrence of Solo deposits is still relevant. Recently, the terrace sequence of the Kendeng has been re-investigated and dated, revealing four terrace levels dating back to the past ~350 ka (Rizal et al., 2020). It makes a re-inventory of the Trinil terraces increasingly relevant.

3. Methods

3.1. Field study

Fieldwork was carried out in 2018 and 2019, studying riverside exposures and sand quarries between Sonde and Ngawi (Fig. 1C and D). We prepared a 12-m resolution digital elevation model (DEM) based on TerraSAR-X/TanDEM-X satellite images (© DLR, 2019) to identify potential terrace surfaces. The surfaces were mapped and surveyed in the field and heights were measured by GPS and referenced with DEM-based heights. In exposures, the build-up of the terraces was studied. Terrace sediments were described and delineated, carefully documenting the position and nature of the contact between terrace deposits and pre-terrace substrate. Correlations between terraces were based on absolute and relative heights of terrace surface and (scour) base and facies of the terrace deposits, bringing to light seven terrace levels. Gravel-composition counts were carried out to obtain an additional parameter for terrace correlations (Supplement 1).

After the terrace deposits were delineated, the pre-terrace stratigraphy was studied in detail. The pre-terrace strata have a slight southward dip (2–10°), which enables the study of stratigraphic sections along north-south directed river transects. Reference sections were selected and described, measured, and photographed. All sites and sections mentioned in the text are indicated in Fig. 1 and Supplement 2.

3.2. Classifications, measurements and protocols

Lithological and textural descriptions are based on Dunham (1962) for carbonates, Wentworth (1922) for epiclastic and Fisher and Schmincke (1984) for pyroclastic material. Deposits are regarded as pyroclastic when they consist for >75% of primary pyroclastic material. This material may be recycled by fluvial processes, but is regarded as epiclastic when eroded from older, consolidated rock. Sand- and silt-sized pyroclastic grains are referred to as ash (unconsolidated) or tuff (consolidated). Gravel-sized pyroclastic clasts are referred to as lapilli. The term lahar refers to volcanic debris flows and to the deposits thus formed. Paleosols have been described following the World Reference Base for soil resources of the Food and Agriculture Organization (FAO, 2015).

The stratigraphic units were originally referred to as Beds (e.g. Trinil Beds). In later publications, these units were re-labeled as Formation (e.g. Kabuh Formation) without further changes to the unit definition.

GPS-measured heights, referenced to the World Geodetic System 1984 (WGS84) have been recalculated to meters above sea level (m + MSL) using a local geoid height of 25.142 m (source: Unavco), i.e. orthometric height (m + MSL) = WGS84 height –

25.142 m.

Our interpretations follow published facies models: Miall (1996, 2014) for fluvial deposits, Ashworth et al. (1994) for braided river deposits, Hampton and Horton (2007) for sheetflow deposits, Cas and Wright (1987) and Fisher and Schmincke (1984) for pyroclastic deposits, Vallence (2005) for lahars, and Tucker (1985) and Wright (1984) for shallow marine carbonates.

3.3. Geochronology

We applied feldspar optically stimulated luminescence (OSL) dating to two representative sediment samples from the fluvial terraces. Details on sample provenance, sampling and measurement protocols and data analyses are provided in Supplement 3.

4. The fluvial terraces and their deposits

4.1. The terrace landscape of Trinil

The plains of Trinil have subtle height differences. Our DEM-analysis distinguished seven terrace levels, with heights ranging between 68 and 50 m + MSL (Fig. 2). All heights represent the situation in the direct vicinity of Trinil. Moving away, terrace heights change, following the gradient of the Solo and as a result of differential uplift. The terrace margins are generally indistinct slopes, remodeled by erosion and rice cultivation. However, at a broader scale, they reflect ancient meander loops and abandoned river courses.

Terraces T7, T6 and T5 form plateaus at 68, 66 and 64 m + MSL. They have sandy surface sediments with rounded gravel and are mostly overgrown with teak forest or sugar cane. T4, T3 and T2 form wide plains, at 59, 58 and 54 m + MSL, covered with rice fields. T4 and T2 have a thin clayey topsoil, overlying a subsoil of consolidated tuffs. T3 has gravelly surface sediment.

The Solo River is deeply incised in this terraced landscape, with wide entrenched meanders. Around Trinil, its gravelly bed lies around 41 m + MSL. T1 forms small terraces at 50 m + MSL, nested along the sides of the Solo incision.

Lehmann referred to the gravel-covered plateaus (our terraces T7, T6 and T5) as the High Terrace. He also recognized T1, along the banks of the current Solo, which he named the Low Terrace. But he remained unclear about the background of the wider plains, which we identified as T4, T3 and T2, probably because he rarely found surface gravel. He left this area blank on his chart, or loosely ascribed parts of the plains to his High or Low Terrace, which is definitely incorrect: The area forms separate terrace surfaces and has a different build-up, as we will show in the next sections.

The tuffs forming the subsoil of T4 and T2 have commonly been described as pre-terrace substrate, either named Trinil Beds (Dubois, 1908) or Kabuh Formation (Duyfjes, 1936), implying that these wide terraces are straths without fluvial surface sediments. This is highly uncommon. Moreover, the wide, relatively low plains do not show signs of extensive surface erosion that could have removed this fluvial cover sediment.

4.2. Sedimentology of T7, T6 and T5

4.2.1. Description

T7, T6 and T5 are made up of fluvial, flat lying surface deposits overlying a planar erosion surface. The latter is easily recognized, running parallel to the terrace surface and truncating the southward dipping substrate. It is covered with an unstructured lag of rounded andesite gravel (thickness 20–60 cm; main gravel size 2–6 cm). Pebbles with red weathering rinds are common

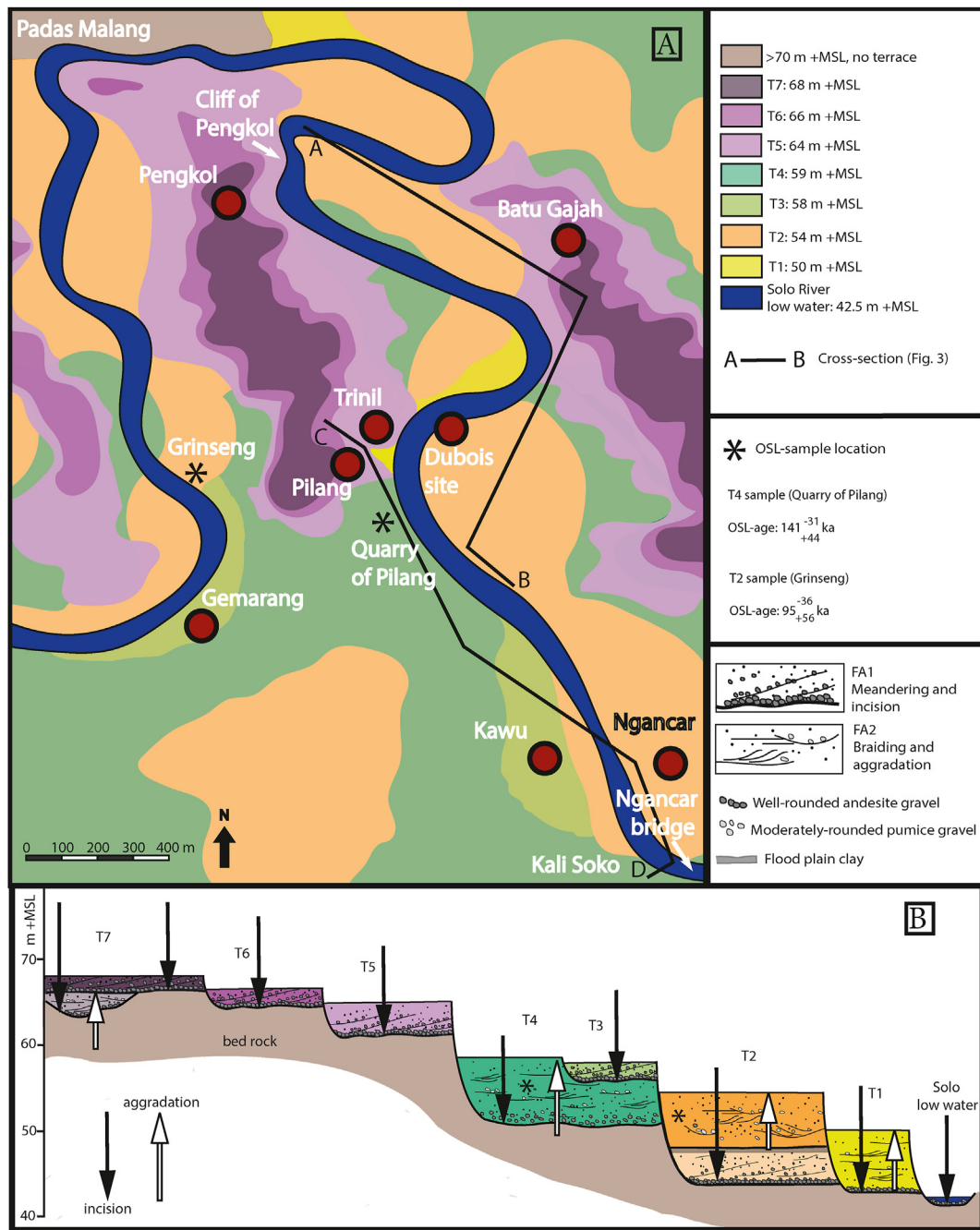


Fig. 2. (A) Map of the fluvial terraces around Trinil © DLR 2019 (TerraSAR-X/TanDEM-X data), (B) Idealized cross-section over the sequence of fluvial terraces of Trinil. FA = Facies Association, see Table 1; OSL datings, see Supplement 3. (For colors the reader is referred to the Web version of this article.)

(Supplement 1). The gravel lag grades into brown-yellow sand and conglomerates with m-scale, low-angle trough cross-bedding structures (Fig. 4, photos 12 and 14). The sand is made up of well-sorted, mono-crystalline (feldspars, pyroxenes, hornblendes) and lithic (andesite) grains. The surface layer of T7 and T6 has a thickness of ca. 2 m, but the T5 sediment locally reaches greater thicknesses. Around the Trinil Museum, its thickness is ca. 4.5 m.

Of special interest are channeled incisions, which are locally found below the T7 planation surface, cutting several meters into

the underlying pre-terrace substrate. The quarries of Batu Gajah and Watugedel (Fig. 3A and C) provide good exposures of such incisions, which are mantled with rounded andesite gravel and filled with greyish-white tuff, dominated by vitric grains and mono-crystalline feldspars. The material has dm-scale trough cross-bedding and stacked channel structures with a lapilli-rich fill dominated by moderately rounded pumice (size range 0.5–3 cm). The strata do not follow the southward dip of the substrate. Moreover, the occurrence of rounded andesite gravel indicates that

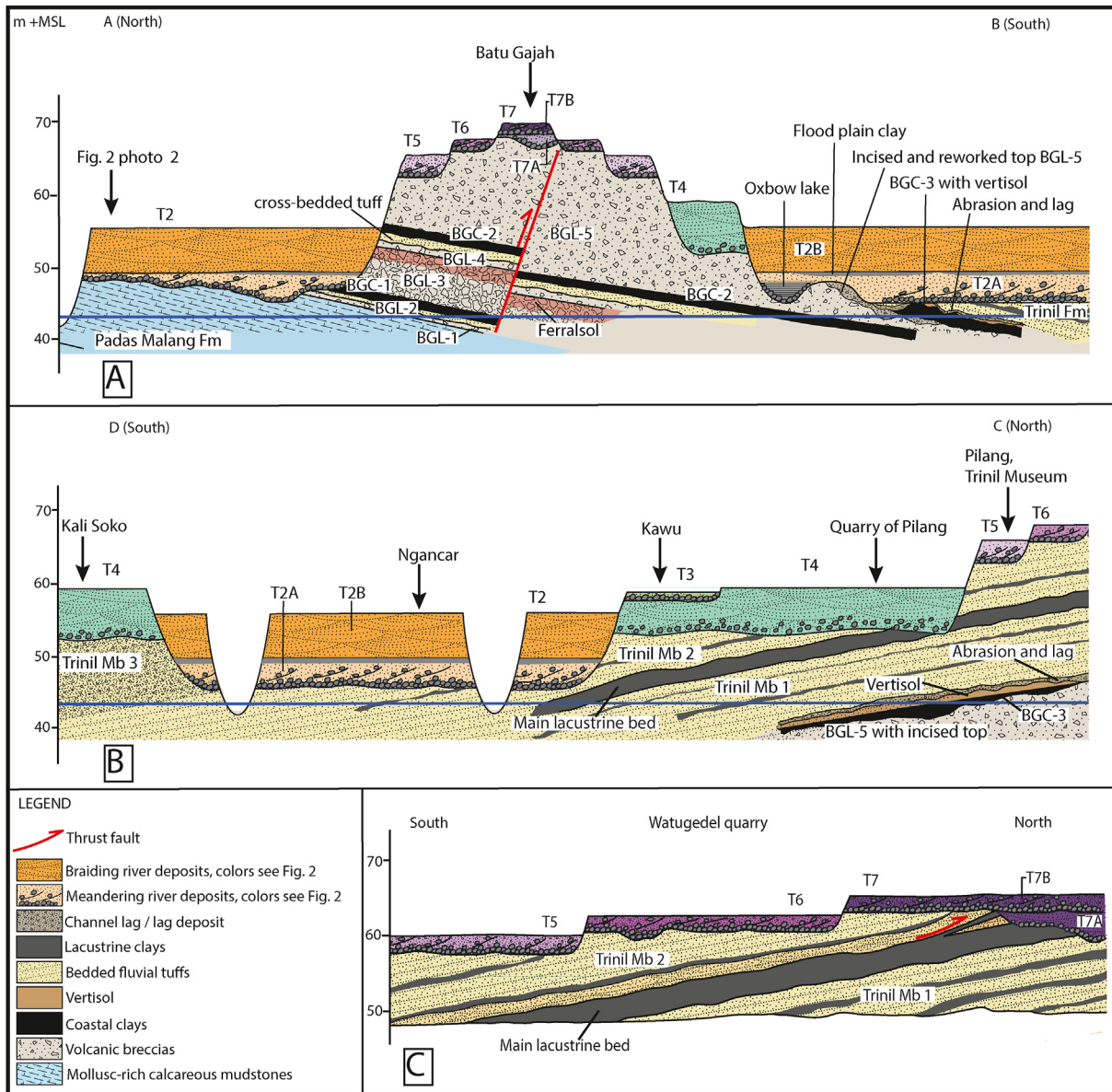


Fig. 3. Cross-sections through the Trinil area, showing schematic occurrence of the stratigraphic (sub)units. Location of the cross-sections are indicated in Fig. 2 and Supplement 2. Colors of the terrace deposits follow the terrace map (Fig. 2). Horizontally not to scale. Section lengths: A and B = ca. 2 km, C = ca. 500 m. Note difference in perspective. The cross-sections follow as much as possible the natural view toward the riverbanks and quarry sides. Note that cross-section A gives a general insight in the stratigraphic situation around the Dubois excavation site. A detailed stratigraphic description of this site will be presented in a separate publication by Hilgen et al. (in prep.). (For interpretation of the references to color in this figure, the reader is referred to the Web version of this article.)

the deposits are part of the terrace sequence. We regard T7 as a composite terrace, made up of two series: T7A and T7B.

4.2.2. Interpretation

T7, T6 and T5 are strath terraces. The gravelly sediment forms a residual mantle, associated with the incisive stage, and represents a laterally mobile gravel-bed river. Lateral accretion structures and a fining-upward grain-size trend indicate meandering conditions. The well-rounded andesite gravel points to long-distance bed-load transport, which is confirmed by its composition, including rock types uncommon in the direct vicinity (Supplement 1).

The relatively thick sediment cover of T5 was formed in conjunction with the gravel-covered scour. We regard this series as a ‘working depth’ deposit of material in transit, representing a situation of simultaneous deepening and widening of the valley

floor (Gibbard and Lewin, 2002).

The channel structures (T7A), locally preserved under the strath of T7B, form remnants of an older fluvial stage. The gravelly lag must be associated with incision, whereas the tuffaceous fill represents subsequent aggradation. The lack of vertical grading and the occurrence of multiple, stacked channels point to braided conditions. The fill was truncated during the subsequent incisive stage of series T7B.

4.2.3. Andesite gravel as a key characteristic of Solo incision

Strath terraces T7, T6 and T5 show that, during its incisive stages, the Solo was a meandering river, carrying a bed load of far-travelled, rounded andesite gravel. The gravel-covered straths form a notable contrast with the underlying substrate, in which we never observed rounded andesite gravel. This raises an important

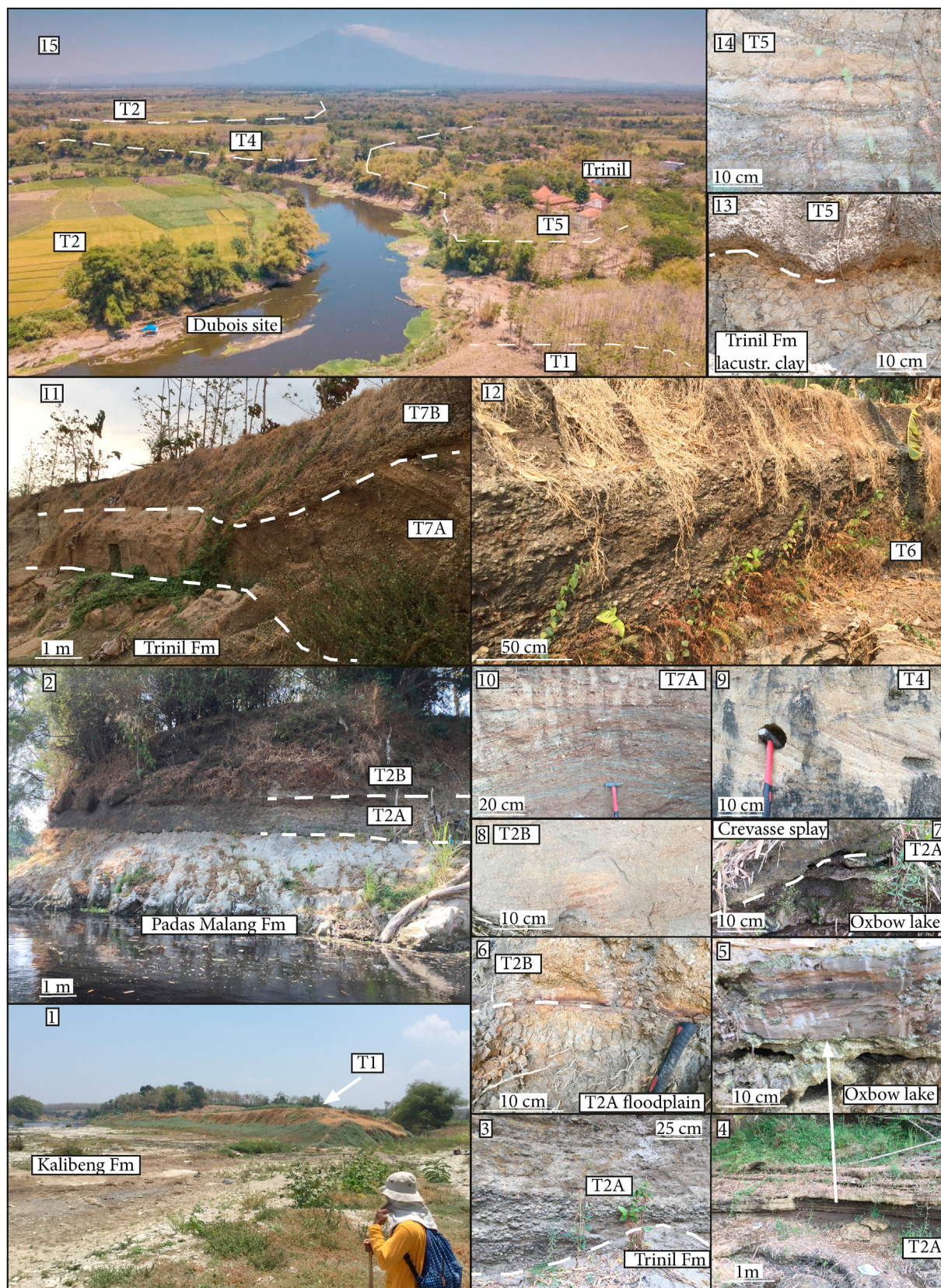


Fig. 4. Selected photographs of the terraces and terrace deposits (Solo Formation). See Supplement 6 for coordinates and setting. (1) Terrace T1, the terrace deposits overlie massive calcareous mudstones (FA3) of the Kalibeng Formation. (2) Terrace T2, terrace deposits T2A and T2B overlying hard calcareous mud bank (FA4) of the Padas Malang Formation. (3) T2A (FA1), channelling scour base and gravel lag over fine tuff (FA11) of the Trinil Formation. (4) T2A, abandoned channel and oxbow lake clays (FA1). (5) idem, zoom in to laminated oxbow lake clays. (6) T2A, floodplain clays (FA1), overlain by cross-bedded ash and pumice (FA2) of T2B. (7) Oxbow lake clays (FA1, T2A), slightly incised and covered with sandy crevasse splay deposits (FA1, T2A). (8) Cross-bedded tuff and pumice (FA2, T2B). (9) Cross-bedded tuff (FA2, T4). (10) Cross-bedded tuff with pumice (FA2, T7A). (11) Terrace T7, T7A

question: Is it possible that the andesite gravel, which Dubois, Van Es and Duyfjes described as interbeds within the tuffaceous Trinil/Kabuh Formation, represent misinterpreted Solo deposits? For this question, the large quarry of Watugedel forms a good reference (Fig. 3 C). It exposes ca. 40 m of planar-bedded tuffs, overlying volcanic breccias. The strata dip ca. 8° to the south, confirming that they belong to the pre-terrace substrate. Dubois (1893), who collected fossils from the nearby Kali Gede, described the strata as the Trinil Beds. The tuffs are mostly planar laminated, rich in in-situ calcareous concretions, and have interbeds of light grey clay. Rounded andesite gravel is absent over the entire length of the section. The dipping beds are truncated by the straths T7, T6 and T5, forming a staircase along the top of the quarry. As expected, the scour surface of the terraces is mantled with rounded andesite gravel. This strongly suggests that rounded andesite gravel is not part of the facies of the Trinil/Kabuh Formation and that andesite gravel is a distinguishing characteristic of a Solo-related incision or planation surface. In the next sections, we will show that this is a valuable field criterion.

4.3. Sedimentology of T4 and T3

4.3.1. Description

The riverside quarry of Pilang provides good exposures of the strata below T4 (Fig. 3B). Dubois and Duyfjes, who referred to the site as Kliteh, described the local tuffs as Trinil/Kabuh Formation. The base of the exposures, just above low water level of the Solo, consists of southward-dipping, planar-bedded fine tuff with in-situ calcareous concretions and interbeds of grey clay.

Halfway up the quarry profile, this dipping series is truncated by a slightly undulating erosional contact, which does not follow the southward dip of the underlying beds, but remains at a height of ca. 51 m + MSL. It is covered with greyish white tuff, consisting of vitric grains and subordinate mono-crystalline feldspars. The series continues up to terrace level and shows trough cross-bedding and stacked channel structures with lapilli-rich fills, dominated by moderately rounded pumice (main size range 0.5–2 cm). The base of this series, up to ca. 1 m above the erosive base, contains dispersed rounded andesite gravel (size range 2–6 cm).

Along the southern edge of the quarry, the surface level steps down ca. 1 m–58 m + MSL. At the same time, a planar scour surface appears at ca. 56 m + MSL, cutting into the T4 sediment. The scour surface is covered with a lag of rounded andesite gravel (thickness 40–70 cm; main gravel size 3–7 cm). The gravel lag grades into brown-yellow sand and conglomerates with m-scale, low-angle trough cross-bedding structures. The sand is made up of mono-crystalline (feldspars, pyroxenes, hornblendes) and vitric grains.

4.3.2. Interpretation

The southward dip of the basal series relates these strata to the pre-terrace substrate. The bedded tuffs are identical to those in the Watugedel quarry and do not contain rounded gravel (Fig. 3B and C). The erosion surface over these strata forms an angular disconformity and marks a previously unnoted stratigraphic boundary. The stacked channels and lack of vertical grading in the overlying fluvial series point to braided conditions and aggradation, whereby the terrace surface appears to form the top of this aggradation stage. Returning to the base of this aggradational series, the dispersed rounded andesite gravel forms a conspicuous element, which we defined in section 4.2.3 as a key characteristic of Solo incision. The gravel does not form a well-defined lag over the scour

surface, as would be expected, but has become dispersed over the lower meter of the tuffaceous fill sediment. We postulate that high-energy currents picked up the gravel during the onset of the aggradation stage.

We conclude that the Pilang quarry exposes two tuffaceous series. A lower, tilted series represents the pre-Solo bedrock. It is truncated by an erosion surface representing Solo incision. The overlying series represents subsequent fluvial deposition, which makes T4 a fill terrace. Previous researchers did not distinguish between the two series, due to their apparently similar composition. However, we do note facies differences: the lower series is characterized by parallel bedding and interbedded clays, whereas the upper, terrace-related series has more dynamic channel and cross-bedding structures. Moreover, the lower series is rich in in-situ calcareous concretions, whereas these were not observed in the overlying terrace-series.

The gravel-covered T3 represents a cut terrace, incising several meters into the fill of T4. Its gravelly surface sediments represent incision and lateral accretion, similar to strath terraces T7 to T5.

4.4. Sedimentology of T2

4.4.1. Description

Moving south from Pilang to the village of Kawu, we descend to terrace T2 (54 m + MSL). The base of the riverbank exposes southward dipping, bedded tuffs, with in-situ calcareous concretions and clayey interbeds, which can be traced back along the river and form the continuation of the material exposed in the base of the Pilang quarry. But here, the bedded tuffs only make up the lower 1 or 2 m of the riverbank profile. At ca. 43.5 m + MSL this dipping series is truncated by a horizontal erosional contact covered by an unstructured lag (thickness 0.1–0.8 m) of rounded andesite gravel (size range 3–8 cm) with admixed reworked calcareous concretions. Locally the gravel is cemented by calcite. The gravel is covered by brown-yellow sand and conglomerate, with m-scale, low-angle trough cross-bedding structures. The sand consists of mono-crystalline (feldspars, pyroxenes, hornblendes) and lithic (andesite) grains. This bedded series fines upward and is overlain by a massive, crumbly dark brown clay, with root traces and red mottling (thickness ca. 0.5 m), the top of which is found at ca. 48.5 + MSL.

The clay is sharply overlain by cross-bedded tuff and fine, moderately rounded pumice lapilli (Fig. 4, photo 6), continuing up to terrace level (54 m + MSL). The tuff is dominated by vitric grains and mono-crystalline feldspars. The series lacks vertical grading and contains multiple, stacked channel structures.

The gravel-covered scour, at ca. 43.5 m + MSL, can be traced along the long river transect between Kawu and Ngancar Bridge, along both banks of the river (Fig. 3A and B). All along this reach, the southward-dipping bedded tuffs, with in-situ calcareous concretions and clayey interbeds, form the lowermost one or 2 m of the riverbank profile, although the southward dip gradually decreases. Interbeds of rounded gravel were not found in this dipping series, confirming our observations in the Watugedel quarry (Section 4.2.3).

4.4.2. Interpretation

The tilted, bedded tuffs, exposed just above low water level, can confidently be regarded as the pre-terrace substrate. Along the long river transect between the Trinil Museum and Ngancar Bridge, these strata form a continuous series reaching a total thickness of

deposits overlain by T7B deposits. (12) Fluvial cover sediment of Terrace 6 (meandering facies, FA1). (13) T5, scour base and gravel lag (FA1) over Trinil Formation. (14) Point bar facies (FA1) of T5. (15) Drone image of Dubois Site (blue tent) and Trinil Museum, with general overview of the terraces.

around 50 m (section 5.3 and 5.4). The erosive surface at 43.5 m + MSL forms an angular disconformity over this series, associated with the overlying terrace T2. The gravel lag marks this scour as an ancient incision level of the Solo. This gravel lag forms the basis of a ca. 5 m thick fining-upward series (T2A), reflecting a gravelly channel, sandy pointbars and floodplain clays. We relate this series to the incisional stage, representing lateral accretion. As we also noted for T5, the relatively thick sediment cover points to temporary storage of material in transit, reflecting ongoing deepening and widening of the valley floor. The thickness of the series corresponds to the depth of the deeper channels on the floodplain (see also section 4.5). The clay layer at ca. 48.5 m + MSL represents the ancient floodplain associated with this laterally migrating river. It has become buried by a second fluvial series (T2B), dominated by tuffaceous sediment. The stacked channels and lack of vertical grading indicate a braided style and aggradational conditions. The terrace surface represents the top of this aggradation stage, which makes T2 a fill terrace. And, as was also noted for T4, the tuffaceous fill of series T2B lacks in-situ calcareous concretions and has more pronounced channel structures than the southward-dipping tuffaceous strata of the pre-terrace substrate, offering valuable diagnostic criteria for distinguishing between terrace deposits and substrate (see Tables 1 and 2, FA2 and FA11).

4.5. The T2-scour over harder substrates

4.5.1. Description

We described the T2 basal scour as a planar erosion surface over the tilted tuffaceous substrate. Along the northern margin of the study area, the pre-terrace substrate is made up of harder lithologies. Here, T2 forms smaller surfaces, roughly following the course of the current river. Often, the basal scour is more irregular. The substrate along the left riverbank opposite the cliffs of Pengkol (Fig. 2) consists of erosion-resistant, cemented calcareous mudstones. These are truncated by a gravel-covered, channeled scour, generally down to an incision depth ranging between 43.5 and 46 m + MSL (Fig. 3A). The incision-related deposits (T2A) consist of rounded andesite gravel overlain by trough cross-bedded conglomerates, only locally capped by floodplain clays. At ca. 48.5 m + MSL, this series is buried by cross-bedded tuffs, forming the aggradational series T2B, which continues up to terrace level (54 m + MSL). Of particular interest are sites where the T2-scour forms isolated channels with a clayey fill, for example along the right riverbank south of Padas Malang and along the left riverbank just upstream of the Dubois site (Fig. 3A; Fig. 4, photos 4 and 5). At

both locations, the T2 scour forms a steep-sided channel, incised in massive volcanic breccias, reaching an incision depth of ca. 43.5 m + MSL. The scour is covered with a lag of rounded andesite gravel, locally cemented by calcite, and forms a conspicuous platform just above low water level. The gravel is sharply overlain by ca. 3 m of light grey, slightly plastic clays with fine silty laminae. The clays are sharply overlain by ca. 1 m of cross-bedded sands, which at their base slightly abrade the laminated clays. Around 48.5 m + MSL, the sand is buried by the tuffaceous, aggradational series T2B, which continues up to terrace level.

4.5.2. Interpretation

The spatial distribution of T2, forming wide plains south of Trinil and narrower surfaces more to the north, reflects variability in bedrock resistance. In the south, the river could easily increase valley width by cutting into the tuffaceous substrate. However, along the northern margin of this abraded platform, abrasion proceeded slower and the river formed more confined channels and meanders. This also explains the relatively thick 'working-depth' deposits of series T2A in more central areas of the former valley floor. The clay-filled, isolated channels represent abandoned channels with oxbow lakes. Silty laminae reflect episodes of flooding of the main channel. The preservation of the laminae indicates oxygen-depleted bottom waters. Trough cross-bedded sands overlying the oxbow-lake clays are part of the basal, meandering-river series and represent flooding events or crevasse splays (Fig. 4, photo 7).

4.6. Sedimentology of T1

4.6.1. Description

The left riverbank east of Padas Malang provides good insight in the build-up of T1. Directly above low water level, the riverbank is made up of marine mudstones. Between 42.5 and 43 m + MSL, these strata are truncated by a planar erosion surface, covered with a ca. 40 cm thick lag of rounded andesite gravel. The erosive contact can be traced along the foot of the terrace, over a distance of several hundred meters. The gravel is sharply overlain by loosely consolidated ash, dominated by vitric grains and monocrystalline feldspars. The series shows fine cross-bedding structures and stacked, shallow channel structures and continues up to terrace surface at 50 m + MSL.

4.6.2. Interpretation

The gravel-covered erosional contact forms a sharp lithological

Table 1
Terrace-related fluvial Facies Associations.

Description	Interpretation
<p>FA1. Planar basal scour surface covered with an unstructured lag (10–80 cm) of clast-supported, well-rounded gravel (size 2–8 cm) (Fig. 4, photo 13). Gravel predominantly of andesitic composition (Supplement 1). Basal gravel covered with ca. 2 m of (fine) conglomerate and yellowish-brown sand with m-scale, low-angle trough cross-bedding (Fig. 4, photos 12 and 14). Sand dominated by mono-crystalline (feldspars, pyroxenes, hornblendes) and lithic (fine andesite fragments) grains. The sand may grade into a top layer of brown, massive clay with a crumbly structure, mottling and fine root traces, but often such fine top layer is absent. Total thickness is generally 2–3 m, up to terrace surface. Locally reaching greater thickness, up to 5 m.</p> <p>Locally, a more irregular basal scour surface occurs, forming deep channels with high-angle banks and thick (up to 80 cm) and coarse (size up to 8 cm) gravel lags (Fig. 4, photo 3). Frequent occurrence of isolated channels cut into the pre-terrace-stratigraphy. Isolated channels may have a fill of plastic, grey, planar laminated clays (Fig. 4, photo 4 and 5).</p>	<p>Incision and lateral accretion</p> <p>Meandering river</p> <p>Material in-transit</p> <p>Partly confined conditions.</p> <p>Oxbow lakes</p>
<p>FA2. Overlying an older scour surface and a lag deposit associated with a previous incision stage, or burying an older terrace. Sediment consists of greyish-white, coarse to fine ash (often consolidated to tuff) with fine, moderately rounded lapilli (size up to 4 cm, main size range 0.5–2 cm). No notable vertical grain-size grading. Ash dominated by vitric grains and fine pumice debris with subordinate mono-crystalline grains (mainly feldspars). Lapilli consist of vesicular pumice and sparse dacites. Frequent occurrence of stacked channel structures, with lapilli-rich fills (Fig. 4, photo 11) and high-angle, dm to m-scale trough cross-bedding (Fig. 4, photos 6 to 10). Outside these channels, the material is generally planar bedded, with fine planar lamination or cross-lamination. Terrace surface is top of aggradation.</p>	<p>Aggradation under high volcanic supply</p> <p>Braided river</p>

contrast with the underlying mudstones and is readily identified as the scour base of T1. It represents the mobile channel-belt characteristic of the incisive Solo. The overlying ash represents a subsequent aggradational stage, characterized by braided conditions, which makes T1 a fill terrace.

T1 follows the course of the current river. Prior to the formation of the recent Solo incision, T1 probably occupied the area of the current channel. Currently, only small plateaus remain along the riverbank. However, patchy remnants of T1-related fill sediment are more widespread, plastered against the lower part of the riverbanks, usually lacking a clear terrace surface. The same accounts for T1-related gravel. Patches of this material occur on the current valley-floor, close to low water level, only slightly higher than the gravel bed of the current river. When studying riverbank exposures, care must be taken to identify such remnants of young T1 sediment.

4.7. Incision and aggradation, fluvial styles and volcanic supply

The terraces of Trinil reflect alternating stages of incision and aggradation, with notable differences in fluvial style. Incisive stages are characterized by gravel-bed rivers. The channel gravel is found in association with overlying point-bar structures and fining-upward sequences, indicating meandering conditions. Also the arcuate terrace margins (Fig. 2) point to a meandering style for the incisive Solo. Aggradational stages are characterized by sediment-laden, braided conditions. Such sequences of meandering incision and braided aggradation reflect changes in the balance of water flow and sediment load. For the Trinil terrace sequence, volcanic supply must have been the decisive factor controlling these changing conditions. The surface sediments of incisional stages consist of epiclastic material, reflecting abrasion and long-distance transport. Aggradational series are invariably made up of fresh pyroclastic material, indicating that stages of braiding and aggradation were triggered by volcanic eruptions.

We subdivided the terrace deposits into two facies associations (Table 1), which are useful for field identification and distinguishing the terrace sediments from the pre-terrace substrate. For the latter, separate Facies Associations will be defined in the section 5.

4.8. OSL dating of the terrace deposits

We selected terraces T2 and T4 for numerical dating, as these fill terraces, unnoted by previous researchers, are of primary interest for the revised stratigraphy of Trinil. We carried out feldspar OSL-dating of the tuffaceous fill of both terraces (Fig. 2). For a detailed discussion on measurement results and interpretations see Supplement 3. The T4 sediment was dated to 141^{+44}_{-31} ka, whereas the T2B sediment was dated to 95^{+56}_{-36} ka. These ages are within the age range of the Solo terraces in the Kendeng Hills around Ngandong, which date back to the past 350 ka (Rizal et al., 2020), confirming that the deposits are part of the Solo terrace sequence and not of the older substrate.

4.9. Correlation between the Trinil and Kendeng terrace sequences

We propose a preliminary correlation between the terraces of Trinil and the terraces of the Kendeng area, based on position within the terrace sequence, composition of terrace sediments and OSL-ages (Fig. 5).

The upper terrace of the Kendeng is a poorly preserved strath terrace with a ca. 1 m thick surface layer rich in rounded andesite gravel (Fauzi et al., 2016). We regard this terrace as the equivalent of Trinil-terraces T7, T6 and T5. Possibly, a detailed study of the

Kendeng upper terrace may reveal a subdivision into (sub)levels, as in Trinil. Referring to the OSL ages of Rizal et al. (2020), we provisionally regard T7, T6 and T5 as a group of straths, with a rough age range of 350–300 ka.

The middle terrace of the Kendeng area can be correlated with Trinil-terrace T4, referring in the first place to their position within the terrace sequence and available OSL-ages. Moreover, the terrace sediment reaches a thickness of >4 m and consists of cross-bedded sand with stacked channel structures, reflecting aggradational conditions similar to T4. An equivalent of terrace T3, cut into the surface of T4, is unknown from the Kendeng area.

The lower terrace of the Kendeng, the famous Ngandong terrace, correlates with Trinil-terrace T2, again referring to their position in the local terrace sequence, the terrace sediment and OSL ages. The lower terrace yielded numerous vertebrate fossils including hominin remains and has recently been extensively re-studied (Huffman et al., 2010; Indriati et al., 2011; Sipola, 2018). The terrace sediment consists of a basal lag of andesite gravel, covered with an aggradational series of pebbly, cross-bedded tuffaceous sands, which the authors relate to contemporaneous volcanic supply, similar to the situation described for Trinil-terrace T2. Rizal et al. (2020) provide multiple dates for the Ngandong lower terrace, indicating an age range of 140 to 92 ka. Our OSL age of series T2B, 95^{+56}_{-36} ka, fits within this range.

Finally, the lowermost terrace of the Kendeng Hills is readily correlated with T1. Both terraces form small surfaces bordering the river, ca. 7 m above low water, and are made up of a thin andesite-gravel lag covered with a fill of unconsolidated ash.

Our OSL ages from Trinil terraces T4 and T2B plot near the lower age range boundary of the corresponding Kendeng terraces, which may be related to differences in applied dating methods. However, it may also reflect differences in timing of the response to degradation or aggradation events along the longitudinal river profile (Bull, 1990).

4.10. Incision and uplift rates based on the Ngandong and Kendeng terraces

The greater heights of the Kendeng terraces compared to the corresponding terraces of Trinil reflect higher uplift rates. Fig. 5B plots Solo incision over the last 350 ka, as recorded by the terraces of the Trinil and Kendeng areas. For the age plots, we used the oldest available OSL ages of the Kendeng terraces, assuming that these provide the closest representation of the incision stage, preceding aggradation.

At Trinil, incision rates were around 90 mm/ka between 350 and 100 ka, slowing down to ca. 10 mm/ka over the last 100 ka. In the Kendeng, incision rates were much higher, reaching values of ca. 200 mm/ka. We regard this prolonged and constant net downcutting of the Solo River as tectonically controlled incision. The greater downcutting rate of the Solo River in the Kendeng Ridge compared to Trinil reflects higher uplift rates (section 7.2). The limited preservation of the Kendeng terraces may very well relate to this higher uplift rate (Veldkamp and van Dijke, 2000).

5. Sedimentology of the pre-terrace substrate

Our careful delineation of the terrace-related deposits made it possible to study the underlying substrate, without the risk of mixing up these two series. We selected four overlapping reference sections (Supplement 2), covering a total thickness of 230 m (Fig. 9). The series has limited lateral variation over the study area. Marker beds are well-identifiable and facilitate correlation between outcrops that may be kilometers apart.

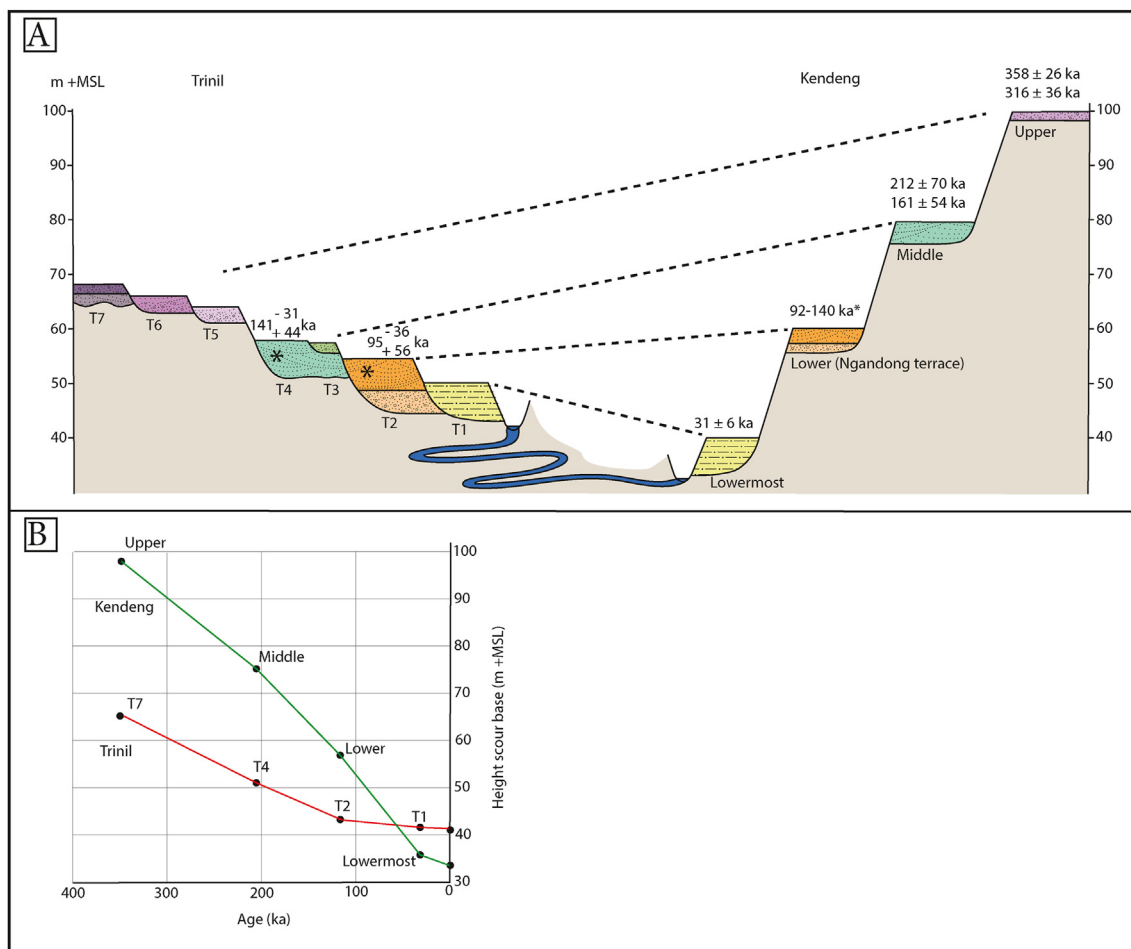


Fig. 5. (A) Correlation between the Solo River terraces of Trinil and the Kendeng Hills with OSL ages. Trinil ages from this study (Supplement 3). Kendeng terrace names and ages from Rizal et al. (2020). * Bayesian modelling including ESR, U-series and Ar/Ar ages. (B) Solo River incision rates over the last ~350 ka for the Trinil and Kendeng areas.

For our descriptions and interpretations, we distinguished 10 Facies Associations (FA3 – FA12) based on texture, sediment composition, sedimentary structures and stratigraphic position (Table 2).

5.1. The Padas Malang Section

The base of the Padas Malang Section forms the lowest stratigraphic level exposed around Trinil. It consists of massive calcareous mudstones (FA3) (Fig. 6, photos 1 and 2). The deposits represent open marine conditions under a low influx of terrigenous material. The rich foraminifera content and thorough bioturbation indicate normal oxygen conditions. The mudstones form the top of a thick marine unit that dominates the exposures of the Kendeng Hills. Correlation with a nearby foraminiferal biostratigraphic section indicates that the strata as exposed around Trinil were formed under outer-shelf depth conditions (Van Gorsel and Troelstra, 1981). Moving upsection, the facies of the mudstones gradually changes, by the introduction of bedding structures and an admixture of granular calcareous material and fine shell debris (Fig. 6, photo 3), reflecting gradual shallowing and increasing energy conditions. Occasional beds are made up of sub-rounded clasts (ca. 10 cm) of calcareous mudstones, indicating nearby erosion of bottom material, likely during storms.

The bedded mudstones grade into mollusc-rich lagoonal deposits (FA4) (Fig. 6, photo 4), reflecting further shallowing. The

absence of bedding structures and presence of abundant burrowing traces indicates a sheltered, lagoonal setting and a limited tidal range, with an estimated water depth of 5–30 m. The frequent occurrence of coral debris indicates nearby coral reefs, but in-situ corals have not been found. A several meter thick interbedded massive, cemented calcareous mudstone is regarded as a mudbank, formed by algae or sea-grasses on the seabed, trapping and binding fine calcareous mud. The mollusc-rich, burrowed strata reach a thickness of ca. 75 m. Moving upsection through these lagoonal strata, the material becomes slightly admixed with fine, vitric ash, pointing to nearby volcanic activity. Gradually the material grades into bedded packstones and grainstones (FA5), representing further shallowing to peritidal conditions, a setting which is confirmed by its stratigraphic position: overlying lagoonal deposits and underlying terrestrial strata. The bedded coarse-grained strata represent high-energy conditions, with turbulent tidal currents and waves supplying calcareous grains and forming ooids. The top of the bedded grainstones, just below a sharp boundary with the overlying terrestrial, non-calcareous deposits, has a crumbly structure, red mottles and contains fine root traces (Fig. 6, photo 11), representing the development of grassy vegetation in an intertidal or supratidal setting.

5.2. The Batu Gajah Section

The Batu Gajah Section covers most of the volcanic breccias of

Table 2
Facies Associations of the pre-terrace series.

Description	Interpretation
FA3. White to light grey, massive calcareous mudstone. No bedding structures (Fig. 6, photos 1 and 2). Rich in well-preserved foraminifera, few diatoms. No macrofossils.	Open marine, outer shelf
FA4. White to light grey, bioclastic wackestone. Fine calcareous matrix with abundant silt or sand-sized calcareous grains and shell debris (Fig. 6, photo 4). Rich in gastropods, bivalves (mostly disarticulated), echinoids and coral debris ^a (Fig. 6 photos 8–10). Well-preserved crustacean burrows (Fig. 6, photos 5 and 6). Locally bedded, but generally massive and strongly affected by bioturbation (Fig. 6, photo 12). Interbeds (1–5 m) of thickly bedded, strongly cemented, greyish white calcareous mudstone with sparse calcareous grains or bioclasts (Fig. 6, photo 7).	Sheltered calcareous lagoon Calcareous mudbank
FA5. Greyish white, bedded packstones and grainstones. Planar bedding (5–30 cm), beds parallel laminated or massive. Sediment made up of sand- to fine gravel-sized calcareous grains, consisting of detrital bioclasts (shell debris and sparse coral debris), ooids and granular calcareous mud. Upward, beds occur with fine root traces and red mottling (Fig. 6, photo 11). Stratigraphic position: overlying the sheltered lagoonal facies (FA5) and underlying terrestrial strata.	Peritidal carbonate platform
FA6. Homogenous black clay, rich in organic matter. Sparse red mottling. Fine blocky structure, slightly plastic (Fig. 7, photos 5 and 12). Contains dispersed fine pyrite crystals (only visible by hand-lens). Occasional fine root traces. Contains occasional, poorly preserved gastropods, assigned to <i>Melanoides</i> aff. <i>tuberculata</i> . The clay forms tabular interbeds with a thickness of 1–3 m between terrestrial volcanic breccias (FA7 and FA8) (Fig. 7, photos 3 and 11).	Coastal marsh
FA7. Massive tuff breccia. Poorly sorted matrix of white-grey, fine to coarse welded tuff, practically devoid of clay. Tuff dominated by vitric and mono-crystalline grains, mainly feldspars and some pyroxenes, with subordinate lithic grains. Contains ca. 20% gravel- to cobble-sized angular fragments and occasional boulders up to 1.5 m. Coarser fragments consist of hard, unweathered (pyroxene) andesite (Supplement 1). Finer fragments (up to 2 cm) dominated by angular, unweathered vesicular pumice (Fig. 7, photos 3, 4, 6, 7). Contains charred wood.	Eruption-induced lahars
FA8. Massive, clayey tuff breccia. Matrix of poorly sorted, grey or brown-red clay, silt and sand (Fig. 7, photos 1, 9, 10, 12). Sand dominated by lithic and crystal grains. Contains ca. 15% gravel-sized, angular to sub-rounded fragments. Diverse clast composition (Supplement 1), most in a soft, weathered state. Contains clay pebbles and uncharred plant fragments.	Slope-collapse induced lahars
FA9. Massive, white to yellow, moderately consolidated fine tuff (Fig. 7, photo 2), dominated by vitric grains. Subordinate crystal grains, mainly feldspar. Top generally fluvially reworked.	Rain-induced ash lahars
FA10. Thickly bedded (m-scale), grey, firmly welded, massive, matrix-supported lapilli-tuff. Hard and compact matrix of poorly-sorted tuff rich in mono-crystalline grains (predominantly plagioclase and pyroxene) with subordinate lithic and vitric grains. Lapilli concentration varies per bed, between 0 and 50%. Lapilli dominated by lithic fragments: sub-rounded dacite (max. clast size 6 cm, main size range 2–4 cm) and subordinate subangular andesite (max. clast size 3 cm, main size range 1–3 cm). Poor in vesiculated pumice. Subtle grading of lapilli gives an indistinct stratification (Fig. 8, photo 11). Interbeds (ca. 50 cm) of fine, wavy-laminated tuff with lenticular structures.	Pyroclastic flows and surges
FA11. Bedded (dm-scale), greyish white fine tuff made up of vitric grains with subordinate mono-crystalline grains (mainly feldspars, occasional laminae enriched in pyroxenes). Beds form sheets with considerable lateral continuity and are generally planar laminated, but occasionally massive, containing fine plant debris. Occasional shallow, low-angle channel structures. Channel fills of coarse tuff with fine, moderately rounded pumice or dacite lapilli and low-angle trough cross-bedding (cm to dm-scale) (Fig. 8, photo 8). Beds often separated by clay drapes or cm-scale massive, grey clay layers with limited lateral continuity. Clays drapes or layers have fine root traces and occasional vertical burrows. Clayey layers contain freshwater molluscs ^b . Most beds contain in-situ calcareous concretions (Fig. 8, photo 3), generally small concentric nodules (up to 6 cm), but locally forming coalescent, platy structures or larger rods (rhyoliths). No notable vertical grain-size trend.	Ash-covered braidplain
FA12. Massive, grey, plastic clay, slightly admixed with fine ash. Contains fine plant debris and freshwater molluscs ^b . The clays are interbedded within FA11, with sharp boundaries. The upper boundary may be slightly incised, or riven by deep desiccation cracks (Fig. 8, photos 8 and 10). Clay beds range in thickness from ca. 50–300 cm (Fig. 8, photos 5 and 6). The beds have a similar composition to the thinner clay interbeds in FA11, but have a considerable lateral continuity. The clays are often found in association with greyish-white, massive or laminated fine ash rich in diatoms. The diatom-rich material contains plant debris and well-preserved leaf imprints (Fig. 8, photos 5, 7, 8).	Shallow lake

^a For species, reference is made to published faunal descriptions (Felix, 1911; Martin, 1909; Staff und Reck, 1911).

^b For species, reference is made to published faunal descriptions (Carthaus, 1911; Joordens et al., 2009; Martin-Icke, H., 1911; Van Benthem Jutting, 1937).

Trinil. Whereas this was previously regarded as one, undifferentiated series, we found that the breccias are made up of several volcanic debris flows (lahars), with differing backgrounds. Following Vallence (2005), we distinguished three types of lahars. Eruption-induced lahars (FA7) have a matrix dominated by juvenile pyroclastic grains and contain <5% clay. They generally start as pyroclastic flows, but change into lahars when they become mixed with crater-lake water or when they enter rivers (Lavigne et al., 2007). Slope-collapse induced lahars (FA8) contain weathered fragments and have a clay-rich matrix (>5%). These lahars are not related to primary pyroclastic eruptions, but to a collapse of water-saturated, weathered and hydro-thermally altered rock making up the slopes of a volcano. The collapse may be initiated by earthquakes or by intrusion of magma or hot gasses into the dome, driving hydrothermal water toward the flanks, resulting in an outward-directed pore-pressure gradient (Scott et al., 2001). Rain-

induced lahars (FA9) are generally low-volume flows of rain-soaked ash, remobilized from surrounding slopes.

The base of the Batu Gajah Section forms a stratigraphic overlap with the top of the Padas Malang Section, consisting of a regressive series changing from lagoonal deposits (FA4) to bedded grainstones (FA5) capped with a rooted top layer of ca. 10 cm. It is overlain by a clay-rich lahar with weathered volcanic fragments (FA8) (Fig. 7, photo 1). The lower boundary of this lahar forms a sharp contact with the rooted top layer of the calcareous grainstones. Except for scarce rip-up clasts, there are no indications of significant abrasion. Although a time-gap cannot be ruled out, the absence of a thicker weathering profile suggests that the debris flow overrode the coastal, grassy landscape.

The breccia is rich in fine plant remains and the matrix has a characteristic reddish-brown color. This indicates that the surface rocks of the upstream volcanic slopes were chemically weathered

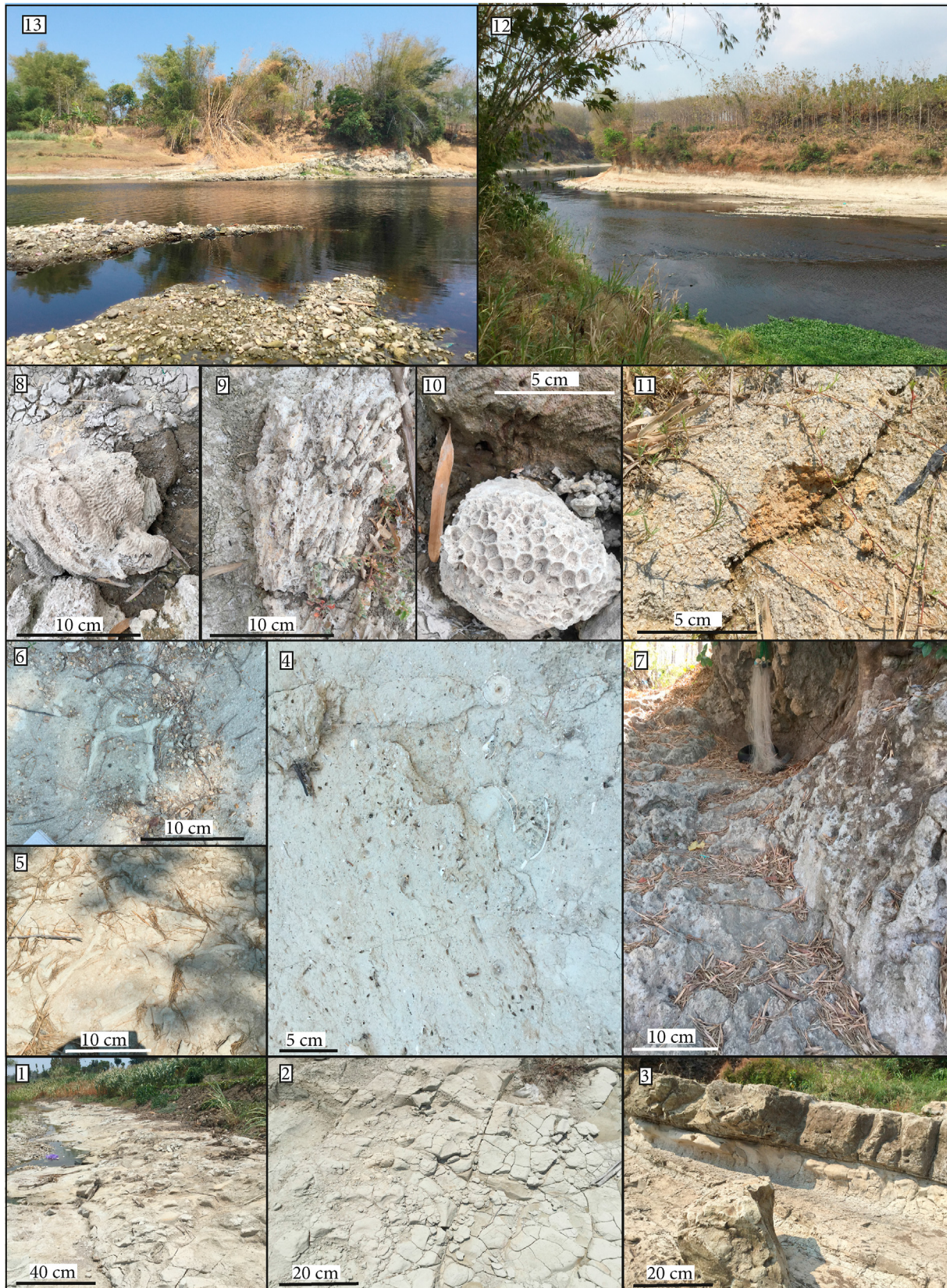


Fig. 6. Selected photographs of the Kalibeng and Padas Malang Formations. See Supplement 6 for coordinates and setting. (1) Massive calcareous mudstones (FA3), Kalibeng Formation. (2) Idem. (3) Bedded mudstones (FA4), base of the Padas Malang Formation. (4) Calcareous lagoon facies (FA4), Padas Malang Formation. (5) Calcareous lagoon facies with burrows (FA4), Padas Malang Formation. (6) Idem. (7) Calcareous mudbank facies (FA4), Padas Malang Formation. (8) Coral rubble bank (FA4), Padas Malang Formation. (9) Idem. (10) Idem. (11) Rooted top layer of bedded grainstones (peritidal facies, FA5), top of Padas Malang Formation. (12) Padas Malang, view on right bank (13) River side exposures of Padas Malang Formation north of Pengkol.



Fig. 7. Selected photographs of the Batu Gajah Formation. See Supplement 6 for coordinates and setting. (1) Clay-rich lahar (FA8) with admixed red-colored ferrallitic weathering material (Batu Gajah Lahar 1). (2) Massive tuff, rain-induced lahar (FA9) with incised top and reworked calcareous concretions (Batu Gajah Lahar 2). (3) Coastal marsh clay (FA6, Batu Gajah Clay 1) overlain by eruption-induced lahar (FA7, Batu Gajah Lahar 3). (4) Eruption-induced lahar (FA7, Batu Gajah Lahar 3). (5) Sample of coastal marsh clay (FA6, Batu Gajah Clay 1). (6) Eruption-induced lahar (FA7, Batu Gajah Lahar 3). (7) Idem, zoom in to matrix. (8) Saprolite (truncated Ferralsol) in the top of Batu Gajah Lahar 3. (9) Remnant of the humic top soil of the Ferralsol along the top of Batu Gajah Lahar 3, overlain by Batu Gajah Lahar 4. (10) Clay-rich lahar (FA8) with admixed yellowish-red ferrallitic weathering

prior to slope-collapse and associated lahar-flow, suggesting humid, tropical conditions. The material contains red, nodular iron concretions (up to 10 cm), which are concentrated along horizontal levels, indicating post-depositional redox accumulations related to groundwater fluctuations. A clayey topsoil associated with this weathering stage is absent, indicating soil truncation.

The basal lahar is overlain by a massive fine tuff layer, representing a rain-induced lahar (FA9) (Fig. 7, photo 2) and reflecting volcanic activity. Its upper surface has been subject to fluvial reworking, as witnessed by ca. 40 cm deep, low-angle channel structures. The channel fill contains reworked calcareous concretions (1–3 cm), indicating a climate with pronounced wet and dry seasons.

A black clay layer (FA6) with a thickness of ca. 2 m overlies the two basal debris flows, (Fig. 7, photos 3 and 5). It forms a laterally continuous marker level that can be traced over the entire study area. The massive and blocky-structured clays indicate thorough bioturbation and intermittent flooding. The clay contains dispersed fine pyrite crystals, which generally form under intermittent brackish water conditions, in combination with high bioavailability of organic matter and a dominant anaerobic environment (Pons et al., 1982; Weaver, 1989; Roychoudhury et al., 2003; Ferreira et al., 2015). This setting is supported by the occurrence of *Melanoides* aff. *tuberculata*, a species common in coastal marshes (Farani et al., 2015). It is interesting to note that coastal marshes with high accumulation of organic matter and pyrite are common in present-day Indonesia (Moormann and van Bremen, 1978). The clay contains a remarkable lens (ca. 60 cm thick) of well-sorted, well-rounded gravel (6–7 cm) with an open structure. The pebbles consist of hard, calcareous material, which must have been eroded from the underlying marine series. Based on their position in the coastal clays and lithological composition, which excludes fluvial supply from the volcanic hinterland, the gravel is regarded as a beach bar.

The black clay layer is sharply overlain by a volcanic breccia (FA7) reaching a thickness of 8–12 m. It has a matrix of white tuff, consisting of partly welded vitric grains and is practically devoid of clay, indicating an eruption-induced background. The underlying clay does not show signs of excessive soil formation, indicating that the lahar directly overran the coastal marsh. The base of the lahar contains wavy streaks of ripped-up clay. The mixed composition of the volcanic fragments points to explosive dome disruption. Vesicular pumice fragments are regarded as juvenile, eruption-related material, while non-vesicular fragments represent older dome rock. The latter includes andesite boulders up to ca. 1.5 m (Fig. 7, photos 4, 6, 7). Charred wood fragments suggest an origin as a pyroclastic flow.

Toward its top, the tuff breccia becomes intensely weathered (Fig. 7, photo 8). The color changes from greyish white to mottled reddish brown and the texture changes from consolidated vitric tuff to crumbly clay. Also the volcanic fragments, still visible in the weathered matrix, have completely altered to clay. Large root traces filled with massive brown clay penetrate the material. The weathering profile has a thickness of at least 3.5 m and represents a regolith. Thin (ca. 20 cm) patches of the humic topsoil have remained (Fig. 7, photo 9), consisting of massive, crumbly, dark brown clay with fine concretions and root traces. It suggests that the original soil profile was a Ferralsol, indicative of a humid tropical climate and well-drained conditions. The largely missing topsoil indicates that the soil profile was truncated. Assuming a weathering rate of 1–2 cm/ka (Evans et al., 2019), the soil profile

represents a timespan of (at least) 175–350 ka.

The paleosol is overlain by a thin clay-rich lahar (FA8) with a characteristic reddish yellow color (Fig. 7, photos 9, 10) that indicates incorporation of soil material in the lahar flow. Referring to the underlying weathering profile, the occurrence of reddish, weathered rock on surrounding volcanic slopes is not surprising. The material contains weathered and unweathered volcanic fragments (generally < 10 cm) consisting of andesite and pumice (Supplement 1). The top of this lahar has been subject to fluvial reworking, as witnessed by low-angle channeling structures with a crudely cross-bedded, poorly sorted fill of a similar yellowish breccia.

The reworked breccia is overlain by a ca. 1 m thick layer of massive, greyish white, poorly consolidated tuff, which we regard as a flow of rain-soaked ash (FA9). The material is poorly exposed and the contact with the underlying reworked breccia could not be observed. Along its top, the tuff is fluvially reworked and well-exposed as a ca. 2 m thick, cemented tuff layer with fine pumice lapilli and dm-scale trough cross-bedding.

The fluvial tuff is sharply overlain by another black clay layer with pyrite crystals (FA6), identical to the clay found lower in the section (Fig. 7, photos 11 and 12), representing a return to coastal backswamp conditions. Again this clay layer, as well as the underlying cross-bedded tuff, forms a well-recognizable marker bed, which can be traced over the entire study area.

The clay is overlain by an up to 15 m thick, clay-rich lahar (FA8) with dispersed angular volcanic clasts of mixed composition: weathered and unweathered pumices, andesites and clay pebbles (Fig. 7, photos 12 and 13). The material is rich in N–S oriented, uncharred logs. The clayey lahar represents a voluminous collapse of water-saturated dome rock, which suggests that the lahar event was triggered by volcanic activity. Fragments of unweathered vesicular pumice in the flow material probably represent syneruptive components. The top of this thick lahar layer is strongly incised, with steep channels cutting meters deep into the lahar surface. The incision surface is covered with crudely cross-bedded, poorly sorted sand and conglomerates, containing semi-rounded volcanic fragments of a mixed andesitic, dacitic and pumice composition (Fig. 7, photo 13).

The incised surface is covered by black clays with fine pyrite (FA6), indicating renewed coastal backswamp conditions. The clay reaches a thickness of several meters and fills the incisions. In the top of the black clay, a ca. 100 cm thick paleosol has formed, reflecting base-level lowering and drainage of the coastal marsh. It consists of pale yellow clay with a blocky structure, red mottles and calcareous concretions (up to 5 cm) (Fig. 8, photo 1). Upwards, slickensides appear, as well as desiccation cracks and small tree-root traces filled with dark grey topsoil material. The weathering profile is characteristic of a Vertisol, pointing to a climate with pronounced dry and wet seasons. The soil profile is truncated and the truncation surface is covered with a ca. 30 cm thick lag of trough cross-bedded coarse ash rich in calcareous concretions. The latter must have been reworked from the eroded soil. The lag deposit is overlain by a thick series of planar laminated fine vitric tuff (FA11).

5.3. The Sogen Section

The base of the Sogen Section mirrors the upper part of the Batu Gajah Section, revealing a remarkably consistent build-up of the stacked series of lahars and interbedded clays. We started our

material (Batu Gajah Lahar 4), (11) Batu Gajah Clay 2 and (overlying) Batu Gajah Lahar 5. (12) Coastal marsh clay (FA6, Batu Gajah Clay 2) overlain by clay-rich lahar (FA8, Batu Gajah Lahar 5). (13) Incised and reworked top of Batu Gajah Lahar 5.

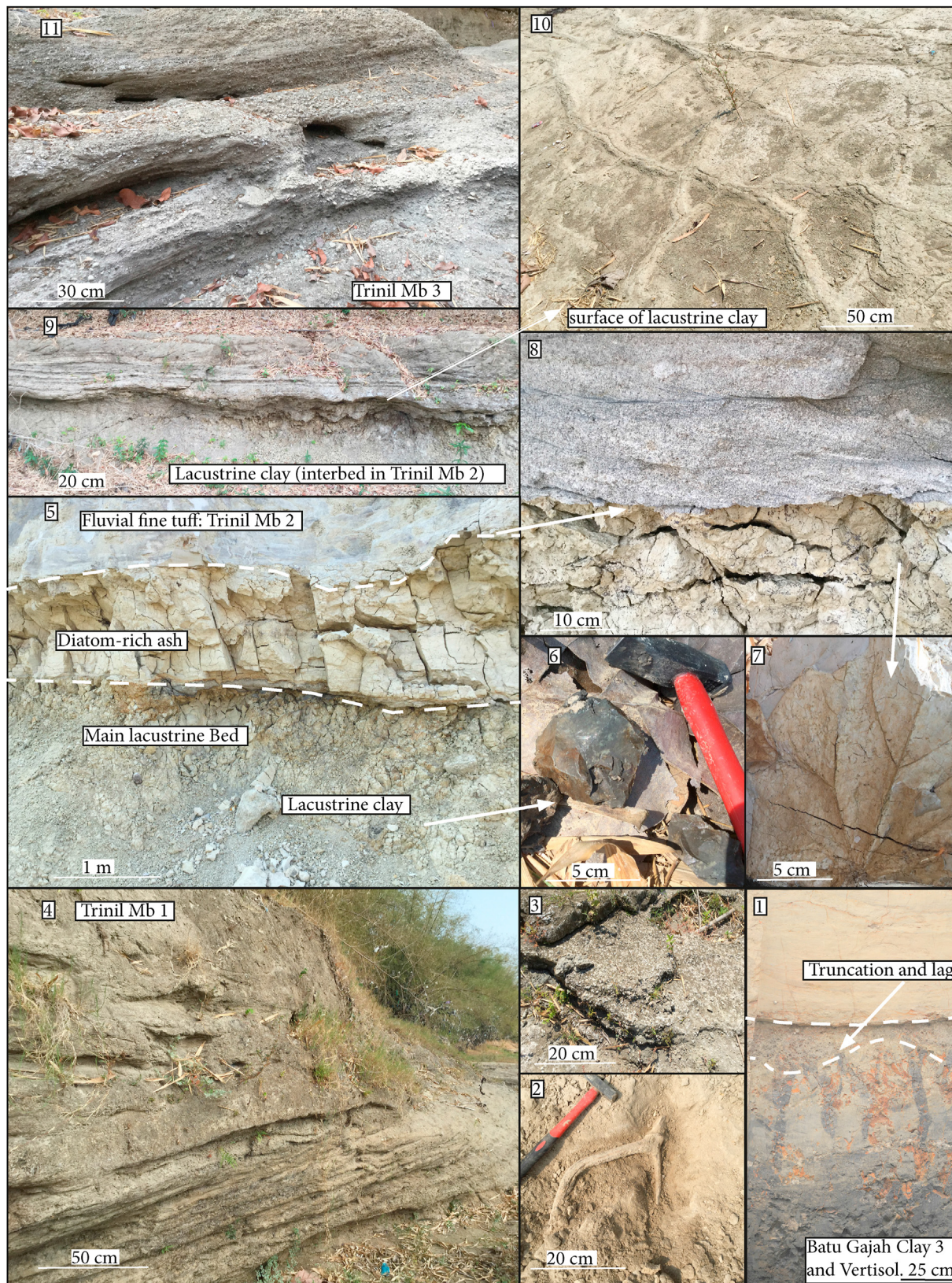


Fig. 8. Selected photographs of the Trinil Formation. See Supplement 6 for coordinates and setting. (1) Batu Gajah Clay 3 with Vertisol, truncation surface and lag deposit, overlain by terrace T1 sediment. (2) Fossil antler (*Axis lydekkeri*) in Trinil Mb 1. (3) Planar bedded tuff (FA11) rich in (in-situ) calcareous concretions (Trinil Mb 1). (4) Planar bedded tuff (FA11, Trinil Mb 1). (5) Lacustrine clay and lacustrine diatomite (FA12, Main lacustrine bed) overlain by fluvial tuff (FA11, Trinil Mb 2). (6) Sample of lacustrine clay (FA12). (7) Leaf fossil from lacustrine diatomite (FA12). (8) Contact surface between Main Lacustrine Bed (diatomite) and overlying tuffs of Trinil Mb 2. (9) Lacustrine interbed in Trinil Mb 2. (10) Top of lacustrine interbed with desiccation cracks. (11) Pyroclastic deposits (FA10, Trinil Mb 3).

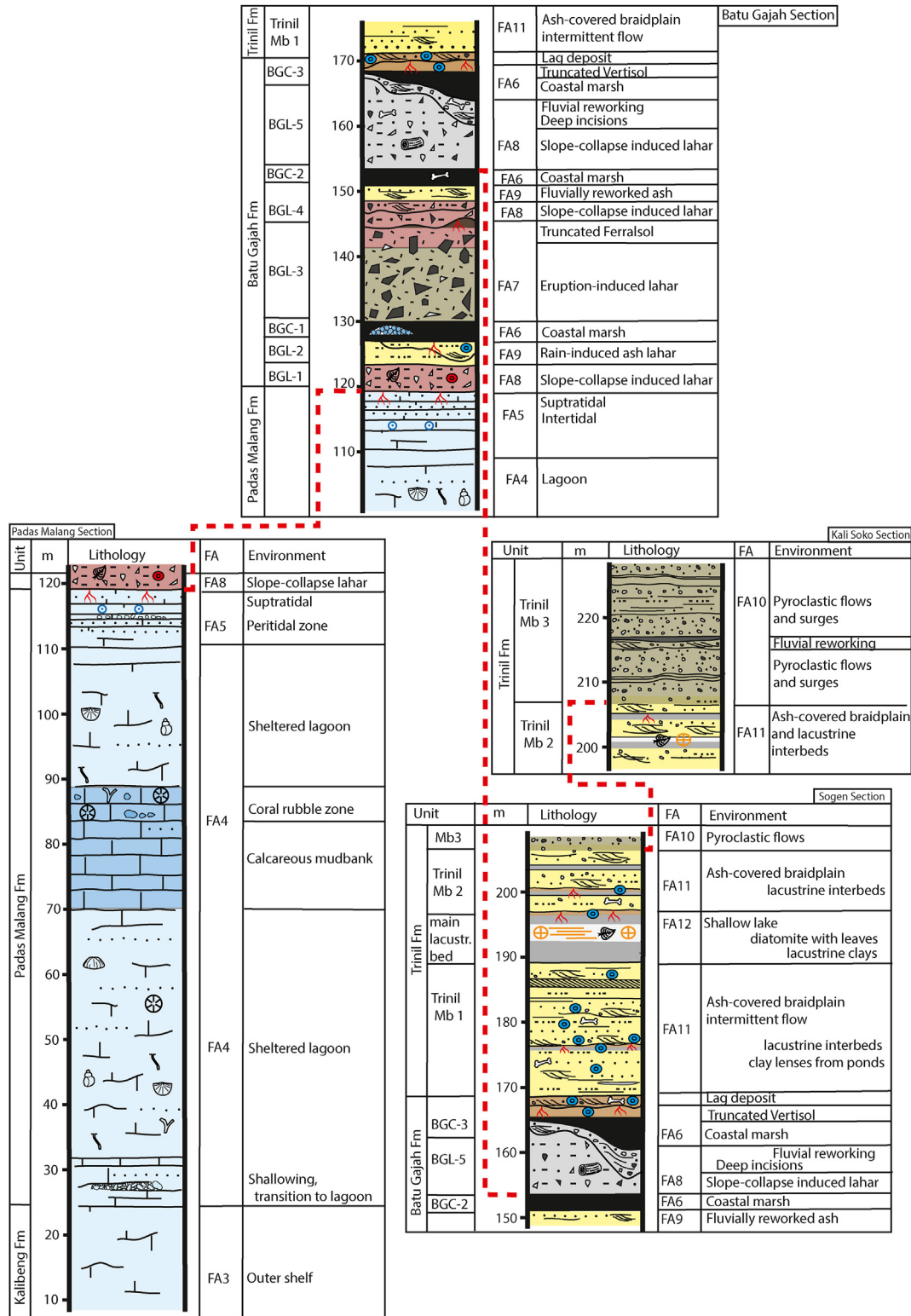
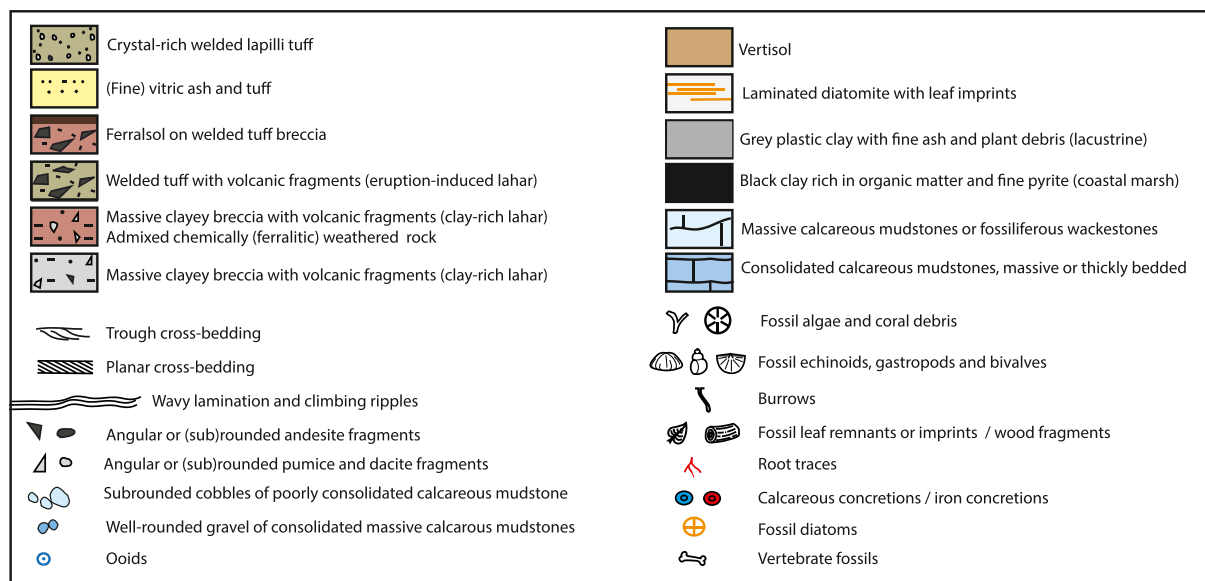


Fig. 9. Pre-terrace stratigraphy of the Trinil area in 4 reference sections, with correlated marker beds. For location of reference sections see Supplement 2. FA = Facies Association, see Table 2. Revised stratigraphy based on this paper. Subunit codes: BGL = Batu Gajah Lahar. BGC = Batu Gajah Clay.



measured section at the base of the thick, clay-rich lahar (FA8) with wood fragments. Again, this lahar is deeply incised and covered with massive black clays (FA6) representing the development of a coastal marsh. The clay contains dispersed fine pumice, which may represent an accumulation of floating pumice, or slumping of slope material from the steep-sided incisions. The clay is capped with a truncated Vertisol, covered with a lag of coarse ash rich in reworked calcareous concretions.

The lag deposit is overlain by a thick series of moderately consolidated planar and locally cross-laminated fine tuff (FA11). The sheet geometry of the beds and planar lamination reflect unconfined, sheetflow-like conditions, with shallow water depths and high current velocities (Fig. 8, photo 4). Occasional shallow channel structures (W: 5–10 m, D: 10–15 cm) represent unconfined, braided channels on the floodplain, with insignificant incision. Cross-lamination, mainly in the channel fills, points to unidirectional, eastward flow. Sheetflow conditions and unconfined braided streams are generally associated with episodic flooding over a wide floodplain (Hampton and Horton, 2007). This setting is confirmed by clay drapes and clay lenses with burrows and desiccation cracks, representing a gradual drying-up of shallow ponds after flooding events. Abundant calcareous concretions indicate a seasonally fluctuating groundwater table or water content, generally associated with pronounced dry and wet seasons (Section 7.5). Horizons with fine rootlets point to a (seasonal) grassy vegetation cover.

The vitric grains and occasional moderately rounded pumice lapilli form juvenile pyroclastic material, indicating a rich volcanic supply. The dominance of well-sorted, fine vitric tuff points to an origin as fallout ash. The material must have been remobilized from surrounding slopes by surface run-off and debris-flows. Interbedded massive, fine tuff layers with plant debris represent small debris flows, which have occasionally been preserved on the floodplain.

The bedded tuffs contain several laterally continuous interbeds of plastic, light grey clays (FA12). The lighter color and absence of pyrite crystals distinguishes these clays from the black coastal marsh clays (FA6). The lighter color relates to an admixture with fine vitric ash and a lower organic content. The absence of pyrite crystals indicates depositional conditions not influenced by intermittent brackish conditions. The clays contain occasional freshwater molluscs, representing stagnant conditions such as lakes or

ponds (Van Benthem Jutting, 1937). The stratigraphic position of the clays, interbedded between sheets of fluviably reworked volcanic tuff, reflects intermittent lacustrine stages (Section 7.6). The plasticity of the clay and the absence of calcareous concretions or mottling indicate that the material was formed under (semi)permanent waterlogging. The massive, well-bioturbated facies rich in plant debris represents a shallow, marginal lacustrine environment or freshwater swamp. The admixture of ash within the lacustrine clays points to ongoing (fluvial) supply of fine pyroclastic material.

The clay interbeds generally have a thickness of 50–100 cm. They may be capped with a thin Vertisol, or have shrinkage cracks along their upper surface, reflecting lake withdrawal. A thicker lacustrine interbed occurs ca. 20 m above the base of the tuff series. The clay layer has a thickness of ca. 3 m and grades into white, massive and laminated fine ash rich in diatoms. The algal blooms indicate nutrient-rich conditions, likely caused by dissolved silica. Increasing eutrophication occasionally led to oxygen-depleted bottom conditions, recorded by non-bioturbated, laminated diatomite (Sáez et al., 2007). The diatomite contains frequent leaf imprints, showing that the lake had forested margins. Euphorbiaceae and Malvaceae tree taxa (Supplement 4) point to a relatively open, sunny tropical forest. Trees of these families are usually pioneering species and are indicative of a disturbed setting (pers. comm. Huang Jian, June 2020). Environmental disturbance may be related to volcanic supply or fluctuating lake levels.

Above this ca. 5 m thick lacustrine interval, the bedded tuff series continues, with frequent interbeds of lacustrine clays (Fig. 8, photo 9). Toward the top of the section, the facies of the tuffs gradually changes: its color becomes greyish as a result of an increasing content of mono-crystalline pyroxenes. Moreover, there is an increasing occurrence of isolated, sub-rounded, low-weight dacite lapilli (up to 3 cm). This announces a more significant facies change in the overlying strata.

5.4. The Kali Soko section

The upward continuation of the bedded tuff series can be observed along the riverbanks south of Padas Malang and south of Trinil. These Solo transects are made up of the same bedded tuff series as the Sogen Section, but the exposures are disturbed by deeply incised terrace bases. South of Trinil, the bedded tuffs are

only exposed in the lower one or 2 m of the riverbank exposures, below the T2 scour surface (Fig. 3B). Approaching Ngancar Bridge, the same facies change can be observed as in the top of the Sogen Section: an increase of monocrystalline pyroxene and admixture of dispersed, moderately rounded dacite gravel. Channel structures become more prominent, reflecting more dynamic flow conditions.

South of Ngancar Bridge, the series can be traced along the banks of Kali Soko (Supplement 2). Its facies gradually changes to grey, matrix-supported lapilli-tuff, with a rhythmic bedding and subtle grading of lapilli (FA10) (Fig. 8, photo 11). This points to deposition by pyroclastic flows rather than water-saturated flows. The matrix is intensely welded, which also points to an origin as hot pyroclastic flows. The richness of lithic lapilli indicates that the pyroclastic flows must be associated with dome explosions rather than rapid vesiculation of magma. The sub-rounded shape of the clasts may be caused by repeated extrusion and fallback in the vent, preceding eruption (Fisher and Schmincke, 1984). Several ca. 50 cm thick interbeds of wavy laminated tuffs are regarded as base surges or ash cloud surges.

Pyroclastic flow deposits were frequently fluvially reworked, as witnessed by channeling structures and dm-scale trough cross-bedding along the top of massive beds. Occasional lenses of clay or fine ash, often with desiccation cracks and fine root traces, represent small ponds. Their upper boundary is frequently convoluted and shows asymmetrical deformation structures, indicating northward-directed shear from overriding pyroclastic flows.

6. Stratigraphic revision

We propose a new, local lithostratigraphy for the Trinil area, with reproducible unit boundaries, following major changes in depositional conditions. Most units have been subdivided into (numbered) subunits.

The relation to the former stratigraphic practice is briefly discussed. Although some of the new units (partly) run parallel to the former units, they should not be regarded as synonyms, because the former units have connotations linked to unfounded regional correlations.

6.1. Kalibeng Formation (revised unit)

6.1.1. Definition

The massive calcareous mudstones (FA3) at the base of the Trinil series are assigned to a redefined Kalibeng Formation.

6.2. Former practice

Duyfjes (1936, 1938) defined the Lower and Upper Kalibeng Formations, consisting of massive calcareous mudstones overlain by diatomaceous mudstones. Berghuis et al. (2019) showed that the diatomaceous strata form a local facies of the larger pelagic series. We therefore propose to discard the prefixes 'Upper and Lower' and regard all pelagic mudstones of the Kendeng Hills as one regional unit: the Kalibeng Formation.

6.3. Padas Malang Formation (new unit)

6.3.1. Definition

We propose the Padas Malang Formation as a new unit for the bedded and/or mollusc-rich calcareous mudstones of Trinil. We define the introduction of bedding structures and the admixture of fine granular calcareous material as the base of the unit. The unit covers all lagoonal and peritidal calcareous deposits up to the first terrestrial, non-calcareous debris flow.

6.3.2. Former practice

Duyfjes (1936) attributed the lagoonal deposits of Trinil to his Upper Kalibeng Formation, correlating the beds with the diatomaceous deposits of the eastern Kendeng Hills. This correlation is incorrect. The diatomaceous strata are significantly older, largely dating from the Early Pliocene, and were formed under bathyal depth conditions (Berghuis et al., 2019).

6.4. Batu Gajah formation (new unit)

6.4.1. Definition

We propose the Batu Gajah Formation as a new unit for the stacked volcanic breccias and interbedded black clays. The sharp contact between the calcareous strata (Padas Malang Formation) and the lowest non-calcareous debris flow forms the base of the unit. The unit continues upwards up to the base of the bedded tuffs. The unit consists of five debris flows, which we numbered Batu Gajah Lahar-1 to 5 (BGL-1 to GGL-5), and contains three interbeds of coastal clay, which have been numbered Batu Gajah Clay-1 to 3 (BGC-1 to BGC-3). The unit contains several paleosols and channelled erosion surfaces, the latter generally covered with a thin lag deposit, representing hiatuses in the depositional record.

6.4.2. Former practice

Duyfjes (1936) attributed the breccias of Trinil to the Pucangan Formation, based on a correlation with the deltaic series of the Jombang area. This correlation is unfounded. The deltaic sandstones of the eastern Kendeng Hills and the breccias of Trinil represent different depositional settings and the age relation between the two series is unknown.

6.5. Trinil Formation (revised unit)

6.5.1. Definition

We propose to return to Dubois' original name, the Trinil Formation, for the bedded tuffs with clayey interbeds. The redefined unit explicitly excludes the terrace deposits. The unit overlies a channelled erosion surface over the Vertisol developed in BGC-3, covered with a lag deposit rich in reworked calcareous concretions. The erosion surface locally cuts through the Vertisol and BGC-3, reaching down into the underlying breccia (BGL-5). We define the contact between this lag deposit and the overlying aggradational series of bedded, fluvial tuffs as the lower boundary of the Trinil Formation. The tuffs reach a thickness of ca. 50 m. A 4–6 m thick layer of lacustrine clays and diatom-rich ash forms a prominent marker bed about halfway within the tuff series. We refer to this level as Main Lacustrine Bed. The tuff series below this marker bed is referred to as Trinil Member 1, the overlying tuffs as Trinil Member 2.

6.5.2. Former practice

Duyfjes (1936) renamed Dubois' Trinil Beds the Kabuh Formation, correlating the deposits with fluvial sands and conglomerates that form the top of the deltaic series of Jombang. This correlation is unfounded: both fluvial series have a different composition, represent a different depositional setting and may very well have a different age. Duyfjes proceeded to define the fossils of Trinil as a distinguishing feature of the Kabuh Formation, which is circular reasoning. Moreover, Duyfjes did not recognize the T2 and T4 terrace deposits and added these strata to the Kabuh Formation, which makes this formation, at least in Trinil, a mixed and invalid unit.

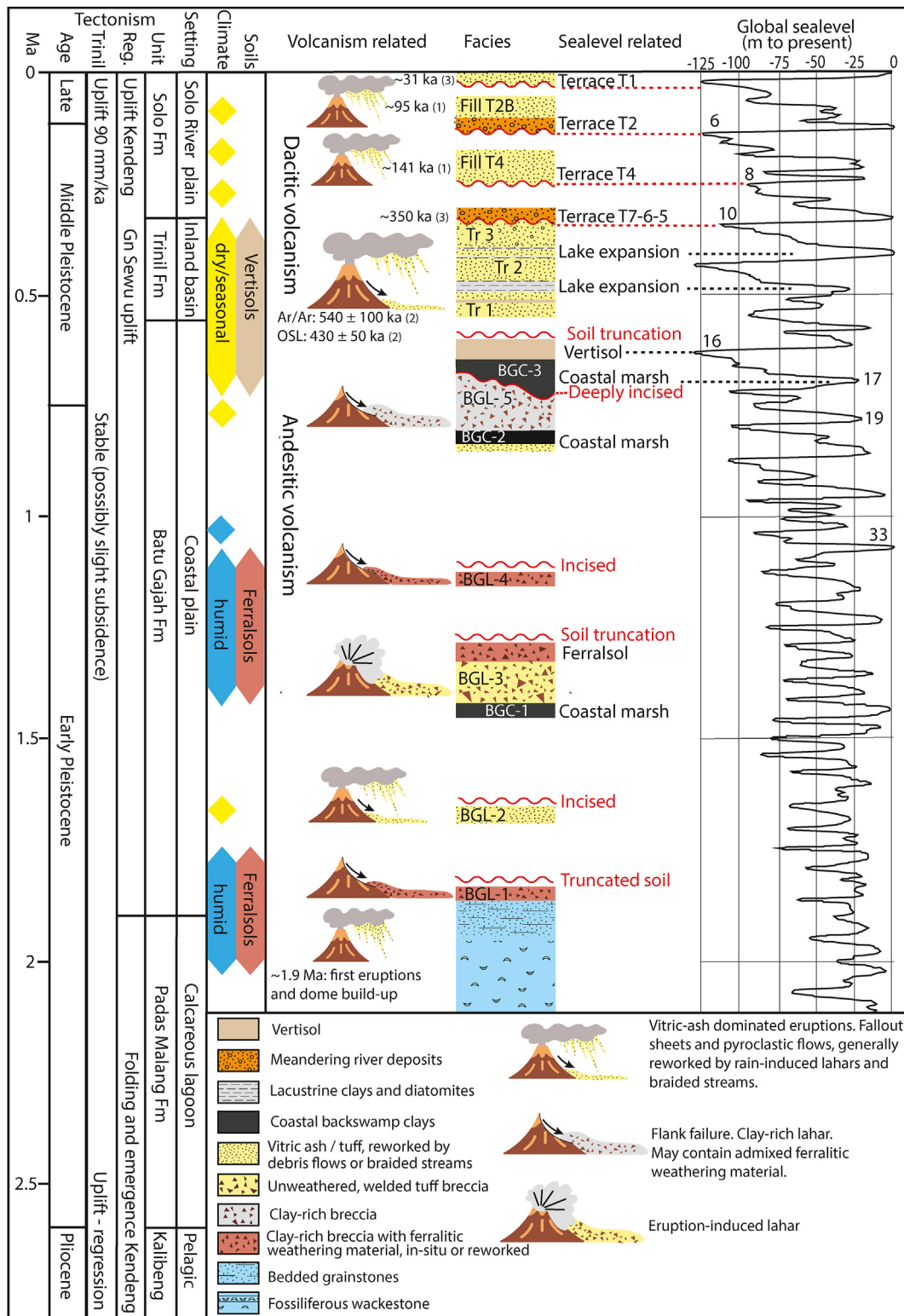


Fig. 10. Stratigraphic summary of the Trinil area in relation to climate, tectonism, volcanism and sea-level fluctuations. Sea-level curve (with Marine Isotope Stages) based on Bintanja and van de Wal (2008). Numerical ages: (1) OSL ages this paper; (2) Ar/Ar and OSL ages from Joordens et al. (2015); (3) OSL ages from Rizal et al. (2020). For colors, the reader is referred to the Web version of this article.

6.6. Trinil Member 3

6.6.1. Definition

We add the lapilli tuffs at the top of the pre-terrace stratigraphy

to the Trinil Formation as a separate member: Trinil Member 3. The deposits form the upward continuation of the fluvial, bedded tuffs. Most of the pyroclastic flows have been fluvially reworked, which compromises an exact definition of the base of this member. We

describe the base of the member as a gradational increase of (lithic) pyroclasts, an increase of grey-colored mono-crystalline grains in the matrix and an increasing occurrence of more prominent channelling and cross-bedding structures. The first preserved pyroclastic flows are found above this transition. Trinil Member 3 has an exposed thickness of ca. 25 m and is covered by younger terrace deposits.

Trinil Member 3 is exposed along the southern margin of the study area. Under the prevailing southward dip, it forms the highest exposed level of the pre-terrace stratigraphy. However, it is possible that the subunit (partly) represents lateral facies change within the Trinil Formation, as the southern exposures may represent the marginal area of the former floodplain, more proximate to the foot slopes of the Lawu.

6.6.2. Former practice

Duyfjes (1936) referred to the lapilli-rich tuffs of the Kali Soko as the Notopuro Formation. For him, the deposits represent a new phase of volcanism-induced deposition, after a long period dominated by fluvial supply of erosion products. This has become an accepted feature within the regional geology (van Bemmelen, 1949). Duyfjes referred to the gravel-bearing terrace deposits of T4 and T2, which he added to the Kabuh Formation. He placed the Kali Soko exposures stratigraphically above the Kabuh Formation and hence noted a change in sediment composition, from abrasion material to pyroclastic material.

6.7. Solo Formation (new unit)

For the deposits of the Solo River, no unit name has been in use. They are generally regarded as alluvium, or locally as terrace deposits. The Solo deposits are of great interest, because of their vertebrate fossils including *Homo erectus*. Moreover, they form an archive of sea-level fluctuations, climate change, tectonism and volcanism, most of which remains unstudied. A separate unit name for these deposits is appropriate. We propose the Solo Formation as a new unit name for all fluvial deposits of the Solo, along the entire river course, either as terraces, valley-fills or floodplain sediments.

6.8. Cross-sections and mapping

The cover of terrace sediments (Solo Formation) complicates geological mapping of the Trinil area. Two stratigraphic sections provide an overview of the occurrence of the newly defined (sub) units in the direct vicinity of Trinil (Fig. 3A and B), illustrating the complex relationship between terrace deposits and pre-terrace strata. The cross-sections partly overlap with the historical cross-sections of Duyfjes (1936) and Carthaus (1911).

Supplement 5 provides a geological sketch map of the direct vicinity of Trinil, excluding the terrace-related cover, and partly overlaps with the map of Duyfjes (1936).

7. Discussion

Fig. 10 provides a stratigraphic summary and a provisional age framework and relates the Trinil series to local or regional tectonism, volcanism, sea-level fluctuations and climate change.

7.1. Age framework

A published planktonic foraminiferal study, carried out north of Ngawi, ca. 10 km from Trinil, provides a detailed age record of the Kalibeng Formation (Van Gorsel and Troelstra, 1981), showing that the unit covers the Late Miocene and Pliocene. The transition to the overlying lagoonal deposits (Padas Malang Formation)

approximates the Pliocene—Pleistocene boundary at 2.6 Ma. The massive mudstones exposed around Trinil form the top of the Kalibeng Formation and hence represent the latest Late Pliocene (~3–2.6 Ma). Up-section, the biostratigraphic signal becomes disturbed because of shallow depositional depths, influencing the occurrence of planktonic species, and an influx of reworked older species. This means that foraminiferal age markers in the Padas Malang Formation must be interpreted with care. Van Gorsel and Troelstra (1981) reported provisional age markers of around 1.9 Ma within this series.

The Batu Gajah Formation represents a significant time span, characterized by lahar events separated by prolonged periods with limited or no sediment accumulation. The lahars indicate the presence of a nearby volcanic dome, most likely the Old Lawu (Fig. 1). The basal lahar Batu Gajah-1 represents slope failure of weathered dome rock, which indicates that it postdates initial dome build-up. Assuming that dome build-up of Old Lawu dates ~1.9 Ma (section 2.1), we provisionally assign an age of ~1.8 Ma to the base of the Batu Gajah Formation. This fits well with the reported planktonic age markers of ca. 1.9 Ma within the Padas Malang Formation. Note that this implies that the earliest Old Lawu eruptions were contemporaneous with the latest lagoonal stage, which is confirmed by admixed ash in the top of the Padas Malang Formation. Little age information is available for the individual lahars of the Batu Gajah Formation. In section 7.4 we will show that tying the Batu Gajah Formation to the global sea-level curve offers a provisional insight into the age of individual subunits. This points to an age of ~600 ka for the Vertisol at the top of the unit, which is in line with a tentative K/Ar age of 0.5 ± 0.3 Ma, reported by Bartstra et al. (1978) for a sample from Batu Gajah Lahar-5. It suggests that the Batu Gajah Formation covers a time span of more than 1 million years.

Joordens et al. (2015) $^{40}\text{Ar}/^{39}\text{Ar}$ -dated detrital hornblende from sediment preserved inside fossil bivalve shells derived from the base of the Trinil Formation, which yielded an age of 0.54 ± 0.10 Ma. OSL measurements on feldspars from the same sediment indicate a burial age of 0.43 ± 0.05 Ma. Together with the constraint provided by the age of ~350 ka for the oldest dated Solo terrace sediments, we assume an age range of ca. 550–350 ka for the Trinil Formation.

The age range of the terrace sequence (Solo Formation) has been well established at 350 ka – recent (section 4.9).

7.2. Tectonism

As explained in section 2.1, the former Kendeng Basin had been subject to uplift throughout the Pliocene. Folding and thrusting of the Kendeng Ridge date from the latest Late Pliocene. This is reflected by the onlap of the Trinil series against the Kendeng Hills, which shows that the Kendeng Ridge stood out as a hill range throughout the Pleistocene. During most of the Early and Middle Pleistocene, the tectonic situation around Trinil was relatively stable and Trinil remained proximate to the sea. The thickness of the local series even suggests slight subsidence, possibly as a result of loading by the cone of the Lawu.

The Solo terraces testify to a second phase of folding and uplift, later in the Middle Pleistocene. In section 4.10 we showed that this uplift stage, which had its focal point in the Kendeng Ridge, dates from the last 350 ka. It can be regarded as a reactivation of the older, Late Pliocene fold zone. The southward dip of the Trinil series, as well as some small-scale thrusts in this series (Fig. 3A and C), must be related to this young tectonic stage.

Duyfjes (1936) and van Bemmelen (1949) also noted this renewed uplift, but dated it 'early in the Middle Pleistocene', referring to gravelly erosion material in the Middle Pleistocene Kabuh Formation. We showed that these gravels are not part of the

tilted substrate, but of the younger terrace deposits.

7.3. Volcanism

Past researchers linked the breccias of Trinil to the volcano Wilis (Carthaus, 1911; Dozy, 1911; Duyfjes, 1936), more than 60 km from Trinil. Lahars travelling such distances are extremely rare and require confined-valley conditions and sufficient gradient (Scott, 1988). We have demonstrated that the lahars of the Batu Gajah Formation were deposited as sheet flows over a wide coastal plain, which points to a more proximal volcanic cone, providing sufficient gradient for a flow to spread out over the adjacent plains. This can only have been the Old Lawu. Wood fragments in lahar Batu Gajah-5, oriented north-south, also point to this volcano as the most likely source.

The volcanic fragments in the lahars of the Batu Gajah Formation indicate andesitic volcanism, which is generally associated with the build-up of high stratovolcanoes with steep slopes. These must have provided the required gradient for the lahars. Most lahars of the Batu Gajah Formation represent slope collapse events of weathered dome-rock. Batu Gajah Lahar-3 is related to primary eruptions and associated explosive dome collapse.

The tuffs of the Trinil Formation mark a drastic change of volcanic style, toward more explosive, gas-rich, dacitic volcanism. The onset of ash deposition over the truncated Vertisol that caps the Batu Gajah Formation, which we have dated to ~550 ka, marks the beginning of this new volcanic phase. We postulate that soil truncation is related to these changing volcanic conditions: massive supply of ash over the wide surroundings of Trinil may have caused a dying-off of vegetation, triggering overland flow and soil erosion. The formation of extensive ash sheets is commonly associated with calderas (Fisher and Schmincke, 1984), but an old caldera has not been identified in the vicinity. It may have become buried under the current cone of Lawu, or it may have been part of the Wilis system, where calderas have been identified (Hartono, 1994).

The oldest terraces T7, T6 and T4 represent incisive, lateral accretion stages under low volcanic supply. The younger terraces reflect alternating stages of abrasion and aggradation, which we linked to intermittent pyroclastic supply (section 4.7). The nearby Lawu is the most likely source.

7.4. Sea-level fluctuations

Since its emergence in the Early Pleistocene, the Trinil area has been in the proximity of the sea. The local sedimentary series bears witness to multiple base-level changes, which can be related to Quaternary sea-level fluctuations. Referring to the available numerical ages, some elements have been tied to the global sea-level curve (Bintanja and van de Wal, 2008) (Fig. 10).

The fluvial terraces represent alternating stages of incision, reflecting changes in external control, e.g. base level, climate, tectonism and volcanic sediment supply. The ages of the terraces roughly follow the 100 ka glacial cycles, suggesting that eustatic sea-level fluctuations were the decisive mechanism controlling downcutting. We provisionally tied the scour surfaces of the most prominent terraces to the lowstands of the last four major glaciations (MIS10, MIS8, MIS6 and MIS2). The tuffaceous sediments of fill terraces T4, T2B and T1 reflect aggradation stages, which were in the first place a response to an increased sediment input related to volcanic eruptions. The OLS ages of terraces T4 and T2 place these aggradation stages in MIS7 and MIS5.

Proceeding downward in the local stratigraphy to the Trinil Formation, we appear to lose the signal of marine base-level changes. The fluvial beds making up this unit are characterized by a great lateral continuity and occasional channel structures are

shallow. This indicates high aggradation rates, but most of all a limited gradient and a stable base level (Miall, 1977, 1996; Hampton and Horton, 2007). The latter is remarkable, knowing that the unit dates from ~550 to 350 ka, a period characterized by high-amplitude sea-level fluctuations. It suggests temporary isolation from the marine base level (section 7.6).

The underlying Batu Gajah Formation was formed on a coastal plain, after the shallow calcareous lagoon, represented by the Padas Malang Formation, had emerged, presumably around 1.8 Ma. The lahars that dominate this unit represent short depositional events, which were separated by prolonged stable periods. The interface between the individual breccia units contains a record of multiple transgressive and regressive cycles. Tabular interbeds of organic clays represent the formation of a stable or slowly aggrading coastal marsh, reflecting highstands. Weathering profiles or incisions of previously deposited breccias most likely reflect lowstands.

The upper layers of the Batu Gajah Formation contain sufficient age-related clues for a tentative linkage to the global sea-level curve. The Vertisol, forming the top of the unit, represents withdrawal of a coastal marsh (represented by Batu Gajah Clay-3). The paleosol underlies the Trinil Formation, to the base of which we assigned a maximum age of 540 ± 100 ka ($^{40}\text{Ar}/^{39}\text{Ar}$) and a minimum (OSL) age of 430 ± 50 ka (based on Joordens et al., 2015). Based on the thickness of the truncated paleosol of more than 1 m and an assumed average weathering rate of 1–2 cm/ka (Evans et al., 2019), the soil represents a weathering period that may have exceeded 100 ka. This makes it possible to place the onset of well-drained conditions in MIS16, at ~650 ka. MIS16 was an extended glacial, with very low sea levels, marking the end of the Mid-Pleistocene transition, when 41 ky glacial-interglacial cycles shifted to larger amplitude 100 ky cycles (Dean et al., 2015). Counting back from MIS16, we may link the coastal clay in which the paleosol developed (Batu Gajah Clay-3) to the highstand of MIS17. This clay overlies the deeply incised surface of Batu Gajah Lahar-5. These incisions reflect well-drained conditions and a low marine base level, which must have preceded the development of the coastal marsh. We tentatively link these incisions to the lowstand of MIS18.

Further downward, the marine base-level record of the Batu Gajah Formation continues, but lacking numerical ages, it becomes impossible to tie this record to the global sea-level curve. Without doubt the sediment record contains significant hiatuses. Depending on the age of Batu Gajah Lahar-5, the underlying Batu Gajah Clay-2 possibly represents the highstand of MIS19 or MIS21.

The thick, eruption-induced Batu Gajah Lahar-3 contains juvenile volcanic material, which offers good possibilities for radiometric dating. It will present future workers with an interesting age marker to link several stratigraphic elements to the sea-level curve: the underlying coastal clay (Batu Gajah Clay-1) and the thick weathering profile in the top of Batu Gajah Lahar-3. This weathering profile represents a long period (or several intermittent periods) of well-drained conditions, reflecting one or more lowstands. Moreover, it forms an important climatological marker (section 7.5).

7.5. Climate

The Trinil stratigraphy represents an interesting record of climate change. Batu Gajah Lahars-1 and -4 have a red-colored clayey matrix, indicating ferrallitic weathering of rocks along volcanic slopes prior to collapse. The thick in-situ weathering profile that formed in the top of Batu Gajah Lahar-3 represents a 175–350 ka timespan of in-situ Ferralsol formation. This shows that humid tropical conditions were dominant during the deposition of the Batu Gajah Formation. Calcareous concretions, found in the top of Batu Gajah Lahar-2, are the only exception to this climatic context

and may represent an interval with a dryer, more seasonal climate.

The thick Vertisol that caps the Batu Gajah Formation represents a climate with pronounced wet and dry seasons. We provisionally linked the withdrawal of the coastal marsh and the formation of this soil profile to the lowstand of MIS16. The actual change from humid to dryer climate conditions may predate this Vertisol. Note that the underlying lahar Batu Gajah-5 is the only clay-rich lahar that does not contain admixed red-colored weathering material. The transition from a humid to a dryer climate may therefore predate this lahar. The Trinil Formation (~550–350 ka) contains abundant indicators of dry and wet seasons, in the form of desiccation cracks, calcareous concretions, horizons with grassy rootlets and interbedded Vertisols.

Our observations are in general agreement with the regional pollen record, which indicates a dominance of tropical forest vegetation throughout the Early Pleistocene (Polhaupessy, 1990; Sémah and Sémah, 2012). The authors noted a transition to more open vegetation types, which they roughly date 'at the end of the Early Pleistocene'. Sémah et al. (2010) noted 'prolonged periods of dry climate' starting around MIS22. Following this conclusion, the thick Ferralsol in Batu Gajah Lahar-3 probably predates MIS22. Open vegetation conditions during the latest Early Pleistocene and the Middle Pleistocene are also inferred from vertebrate fossils, which are dominated by large herbivores (Van den Bergh et al., 1996, 2001) and from oxygen isotope signals in herbivore teeth, indicative of grazing on C_4 vegetation (Janssen et al., 2016; Louys and Roberts, 2020; Puspaningrum et al., 2020). Moreover, on a regional scale, Denell (2009) noted an increasing length and intensity of dry periods in Asia during the Mid-Pleistocene Transition.

Several authors noted a change to more humid conditions in eastern Java in the Late Pleistocene, probably postdating the formation of the lower terrace of Ngandong (Van den Bergh et al., 1996; Rizal et al., 2020). This climate change likely affected erosion and sedimentation patterns of the Solo, which may have been recorded in terrace T2 and T1 and forms an interesting subject for future, detailed studies of these terraces.

7.6. Middle Pleistocene isolation: the Ngawi lake basin

The absence of a record of marine base-level changes in the Trinil Formation and the occurrence of lacustrine interbeds points to temporary isolation. The deposition of this unit coincided with a sharp increase of volcanic activity of the Lawu, suggesting that isolation was caused by a volcanic barrier. In section 5.3 we described the depositional setting of the bedded, predominantly planar laminated tuffs as a wide floodplain with a limited gradient. The climate of dry and wet seasons caused events of peak discharge, supplying abundant unconsolidated fine ash to the floodplain. Ash-covered surfaces have a poor permeability, favouring flashy sheetflow and unconfined braided flow (Paredes et al., 2007).

Paleocurrent observations in the fluvial tuffs of the Trinil Formation indicate stable, unidirectional flow, directed to the north-east in exposures around Trinil and to the southeast in exposures around Pitu and Sogen. This eastward paleocurrent was also noted by Dubois (1894b, 1908). We postulate the existence of a Middle Pleistocene lake, which must have been located east of Trinil. In this model the lacustrine interbeds as found around Trinil, form a record of lake expansion and retreat, probably representing fluctuations in precipitation rate. On the Sunda Shelf, sea-level highstands are generally related to increased precipitation rates (Heaney, 1991; Van der Kaars et al., 2000; Bird et al., 2005). The Main Lacustrine Bed of the Trinil Formation may relate to the highstands of MIS13 and MIS11.

The eastward paleocurrents point to a hydrological barrier that

must have been located west of Trinil. Looking at the current landscape, we note that east of Sonde, the lower slopes of Lawu stretch out toward the Kendeng Ridge. This may form a remnant of a Middle Pleistocene barrier, which separated Trinil from the marine base level.

Our study is the first to document the former existence of a lake basin around Trinil (~550–350 ka), which we refer to as the Ngawi Lake Basin. This provides a new view on the habitat of *Homo erectus*. During the long dry seasons that characterized eastern Java throughout the Middle Pleistocene, the tree-lined lake must have provided good living conditions for an early human population, yielding molluscs, fish and drinking water, and attracting game.

7.7. A new model for the development of the Solo

The development of the Solo River marks the end of the Ngawi Lake Basin. Several authors have written about the origin of this river and its remarkable course, crossing the island from south to north. Lehman (1936) and Pannekoek (1949) described an abandoned valley through the Gunung Sewu, which they regarded as an old, southward course of the Solo. Further uplift of these hills and associated blockfaulting would have caused flow reversal, whereby the river forced its new route through the Kendeng Ridge. This is an unlikely representation of river behavior. Moreover, Rizal et al. (2020) dated Gunung Sewu uplift to ~550 ka, which implies a 200 ka time gap with the development of the oldest Solo terraces, dated to ~350 ka.

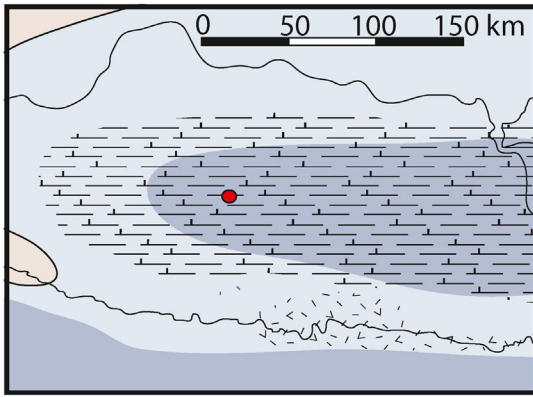
We noted in section 7.6 that in the Ngawi Lake Basin an eastward-directed drainage system developed, toward a lake east of Trinil. It is noteworthy that this drainage was parallel to the later Solo. Westward directed, headward erosion of these streams must have gradually cut through the volcanic barrier west of Trinil. We postulate that by ~350 ka, the headwaters of these streams connected to the plains in the west and captured the local southward directed drainage system (the 'Old Solo'), creating a large, eastward-flowing river system. Similar examples of river capture have been described in other volcanic areas, where rivers were temporarily blocked (Maddy et al., 2012; Veldkamp et al., 2012).

This model for the development of the Solo River also sheds a new light on the river's remarkable traversal of the Kendeng Hills. It may have formed as a northward-directed overflow of the former lake. The current transverse valley still reflects its original meandering course. By the time the eastward draining Solo had developed, the former lake overflow had been incorporated in the river's course.

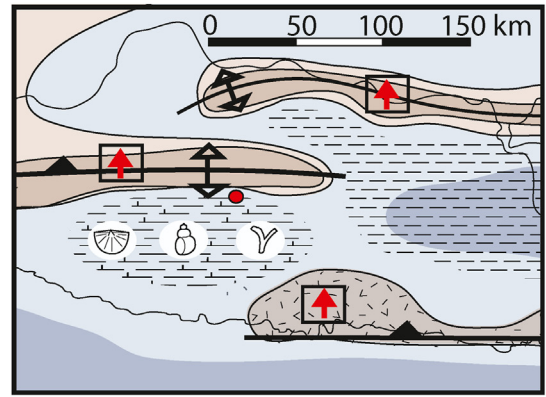
7.8. Landscape reconstructions (Fig. 11)

The Kalibeng Formation bears witness to the marine Kendeng Basin and records regressive conditions throughout the Pliocene. Ongoing compression of the basin sediments formed east-west directed fold and thrust zones, emerging by the end of the Pliocene. Emergence of the Kendeng Ridge left a sheltered, shallow marine lagoon along its southern slopes. The deposits from this lagoon constitute the Padas Malang Formation.

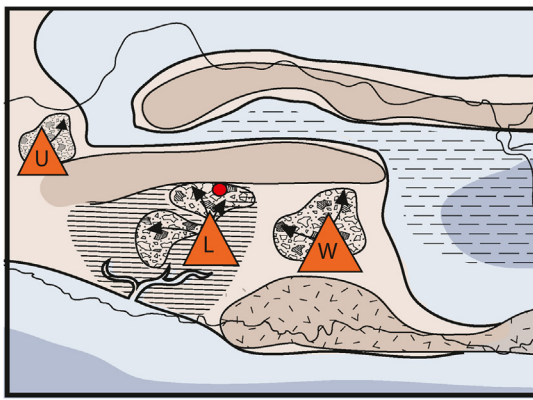
Lawu developed as an andesitic stratovolcano with steep slopes. The lagoon gradually emerged and a coastal lowland developed, at the foot of Lawu. The plains were occasionally overrun by volcanic debris flows, but such events were separated by prolonged, stable periods. During highstands, muddy, organic-rich coastal marshes developed, which form a contrast with the earlier calcareous lagoons. This reflects an increased supply of acidic river water and fine clastic material to the coastal environment, which points to a larger catchment with weathered soils and/or increasingly humid conditions. During lowstands, the area was subject to incision and



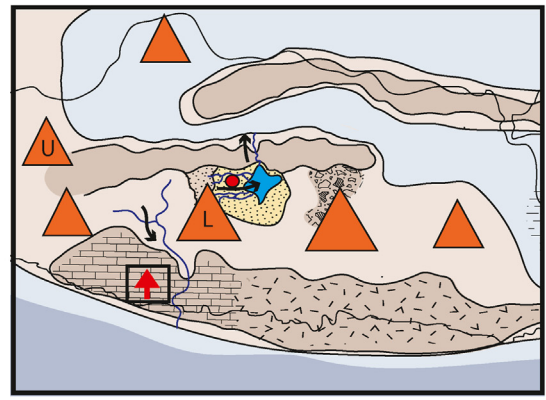
Late Pliocene. Kendeng Basin. Regressive.
Kalibeng Formation



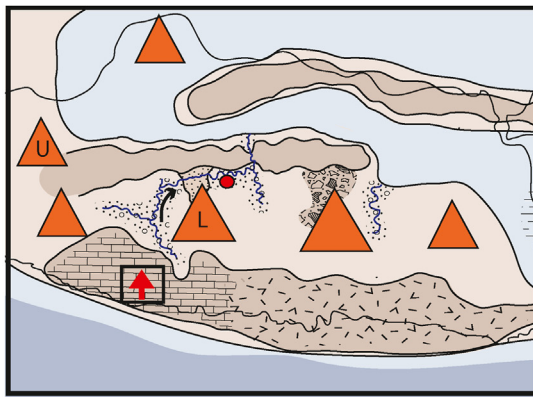
Early Pleistocene ~ 2.6 - 1.8 Ma.
Padas Malang Formation



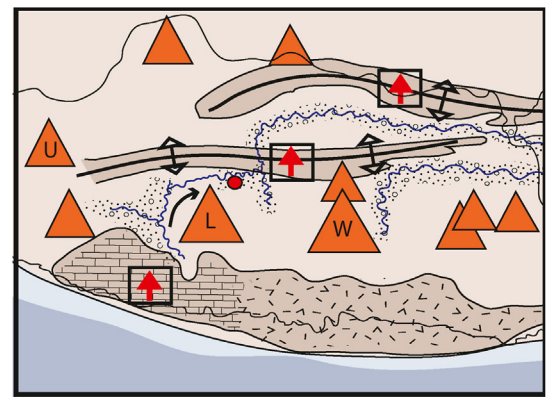
Early Pleistocene ~1.8 - 0.6 Ma.
Batu Gajah Fm. Sea-level highstand.



Middle Pleistocene ~ 550 - 350 ka.
Trinil Formation. Sea-level highstand.



Middle Pleistocene ~350 ka.
Solo Formation. Sea-level highstand.



Middle to Late Pleistocene 350 ka - recent.
Solo Formation. Sea-level lowstand.

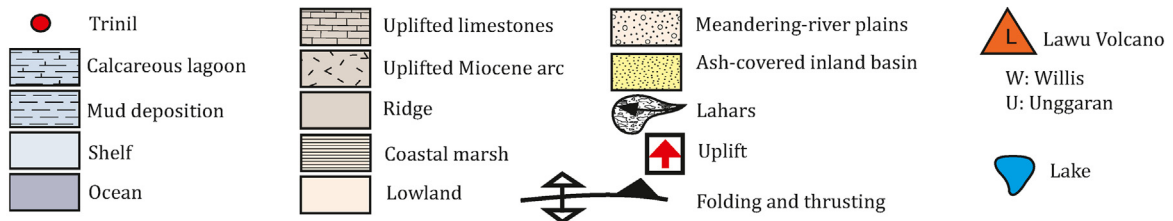


Fig. 11. Plio-Pleistocene paleogeography of Trinil and adjacent parts of eastern Java. Thin black line: outline of present-day eastern Java. Partly based on Huffman et al. (1999), Lunt (2013) and Berghuis et al. (2019).

weathering. Ferralitic weathering indicates humid tropical climate conditions. A Vertisol at the top of the Batu Gajah Formation indicates that, by this time, the climate had become dryer, with marked dry and wet seasons. The complex of volcanic debris flows, interbedded coastal clays and weathering profiles constitutes the Batu Gajah Formation.

At ca. 550 ka, the volcanic regime changed from andesitic to dacitic. Explosive volcanism supplied large amounts of vitric ash and fine pumice. A volcanic barrier developed, isolating the plains of Trinil from the marine base level and creating a lake basin. The area became an ash-covered inland plain, with dry, strongly seasonal climate conditions bringing about peak discharges, with sheetflow and shallow braided flow conditions. Drainage was eastward, towards a lake in the lowest part of the plain. The ash-covered plains had a grass-dominated vegetation, but the lake margins were forested. Lake expansion and retreat reflected fluctuations in precipitation rate. Possibly, the lake developed a northern overflow through the eroded remains of the Kendeng Ridge. The ash-dominated fluvial deposits with lacustrine interbeds constitute the Trinil Formation.

Around 350 ka, headward erosion of eastward-flowing streams inside the lake basin connected to the plains west of the volcanic barrier and captured southward-flowing rivers, creating a large, eastward-flowing river system: the Solo. This reconnected the Trinil area to the marine base level, but this time to the north.

The development of the Solo coincided with renewed uplift. Stepwise fluvial downcutting was predominantly controlled by marine base-level changes. This is unsurprising, as the shoreline was in the immediate proximity. The Randublatung Basin, north of the Kendeng Ridge, contains a record of Middle to Late Pleistocene shallow marine clays (Pringgoprawiro and Baharuddin, 1979) and fluvial, Solo-related sediment bodies (Bartstra, 1988), indicating that this lowland was inundated during highstands and formed an extension of the Solo floodplain during lowstands.

8. Retrospective

Our reinterpretations of the Trinil series are primarily based on advances in the field of sedimentology and Quaternary geology and do not disqualify the work of earlier geologists. Although previously regarded as contradictory, many of their interpretations were valid and found their way into our new depositional model of the Trinil Formation, such as fluvial deposition (Dubois, 1907), interbeds of rain-induced volcanic debris flows (Volz, 1907; Dozy, 1911) and shallow lacustrine deposits (Carthaus, 1911; Dozy, 1911). Also Van Es (1931) and Duyfjes (1936) were correct in their interpretation of fluvial conglomerates as erosion products, representing uplift. But they did not note that this material is a younger deposit, related to the terraces. When it comes to the relation between the older tuffs and the overlying terrace deposits, the hypotheses of Elbert (1908) and Bartstra (1982) were surprisingly accurate. Dubois (1908) fiercely rejected Elbert's idea, but his criticism may have been prompted by fear that this would degrade his fossil collection to a mixed assemblage. Lehmann (1936) correctly identified fluvial terraces around Trinil and understood that these are related to the terraces of the Kendeng, but he did not recognize the full terrace sequence and erroneously suggested that his High Terrace (in this paper T7, T6 and T5) is the equivalent of the fossiliferous terrace of Ngandong.

9. Conclusions

The plains of Trinil form the ancient floodplain of the Solo and are shaped as a terraced landscape. During incisive stages, the Solo deepened and widened its valley floor, under gravel-bearing,

meandering conditions. Intermittent stages of high pyroclastic supply triggered a change to aggradation and braided flow. Stable uplift and intermittent conditions of incision and aggradation formed a sequence of strath and fill terraces. The terraces range in age from ~350 ka to ~30 ka and correlate with the terraces of the Kendeng Hills, ca. 20 km downstream. The tuffaceous sediment of fill terraces T4 and T2 was previously not recognized as terrace-related and was added to the Kabuh Formation, confounding sedimentological and stratigraphic interpretations. We reject the use of the regional unit Kabuh Formation in the Trinil area, and regard the local tuffs as belonging to either the Trinil Formation (substrate) or the Solo Formation (terrace deposits). This has great consequences for the validity of local fossil assemblages and their ages, as most fossils reportedly derive from the Kabuh Formation.

The exposed pre-terrace series has a thickness of 230 m and covers a period from ~3 Ma to ~350 ka. We subdivided the series into four new or revised lithostratigraphic units, representing distinctive depositional landscapes. Our revised stratigraphy forms a local framework and the units should not be synonymized with the existing regional units of Duyfjes (1938). The (chrono)stratigraphic relation with other famous hominin sites in eastern Java, such as Sangiran and Mojokerto, is complex and awaits further studies.

Our landscape reconstructions provide a new view on the habitat of the Middle Pleistocene *Homo erectus*. A lake basin (~550–350 ka) provided the 'fortunate conditions' (Dennell, 2009) required for an enduring presence of *Homo erectus*. In the subsequent stage, this role was taken over by the perennial Solo.

The Trinil depositional series forms an interesting record of Pleistocene tectonism, volcanism, climate change, sea-level fluctuations and fluvial architecture, which gives it regional significance, for Java and maritime Southeast Asia. On a local scale, our stratigraphic revision forms a much-needed basis for a re-evaluation of Dubois' and Selenka's excavation sites and the Trinil fossil assemblages, which will be addressed in a separate publication.

Declaration of competing interest

The authors declare that they have no known competing financial interests or personal relationships that could have appeared to influence the work reported in this paper.

Acknowledgements

This study was carried out with permission of the Indonesian Ministry of Research, Technology and Higher Education (RISTEK research permits: 263/SIP/FRP/ES/Dit. KI/VII/2016 of Josephine Joordens; 284/SIP/FRP/E5/Dit.KI/IX/2018 and 343/E5/E5.4/SIP/2019 of Harold Berghuis) under the project 'Studying Human Origin in East Java'. We thank Arkenas and in particular Dr. I Made Geria for facilitating our inspiring and enduring cooperation. We are grateful to the people of Trinil, Kawu and Ngancar, and to the staff of the Trinil Museum for their hospitality and support. We thank our collaborators and assistants Catur Hari Gumono, Agus Hadi Widiyanto, Suwono and their team, and the research team of the Sangiran Museum for the pleasant cooperation in the field. We thank David Bridgland for his advice and extensive review of the manuscript. We thank Huang Jian for his leaf identifications and Frank Huffman for his critical remarks on our work. The fieldwork was funded by the Treub Foundation (Maatschappij voor Wetenschappelijk Onderzoek in de Tropen), the Faculty of Archaeology, Leiden University and the Dutch Research Council NWO (Grant number 016. Vidi.171.049).

Appendix A. Supplementary data

Supplementary data to this article can be found online at <https://doi.org/10.1016/j.quascirev.2021.106912>.

Author contributions

HB, AV, and JJ designed the study. TS initiated the overarching research project and together with SA and DRE ensured embedding within the Indonesian research infrastructure. HB directed the field study and analysis of the stratigraphic data, and wrote the manuscript. AV, SA, SH, IS, DHB, EP, DY, DRE, HB, TvK and JJ participated in the field study and analysis of the data. TR and SH conducted the OSL dating. AV and JS interpreted Digital Elevation Models and reconstructed the fluvial terrace landscapes. JJ and SA are the Principal Investigators of the research project. All authors contributed to writing, reviewing and final approval of the manuscript.

References

- Ashworth, P.J., Best, J.L., Leddy, J.O., 1994. The physical modelling of braided rivers and deposition of fine-grained sediment. In: *Process Models and Theoretical Geomorphology*, Wiley and sons, Chichester, pp. 115–139.
- Bartstra, G., 1982. The river-laid strata near Trinil, site of *Homo erectus*, Java, Indonesia. *Mod. Quat. Res. Southeast Asia* 7, 97–130.
- Bartstra, G.-J., 1988. The age of Solo man and Java man. In: *Early Man in the Southern Hemisphere*, pp. 12–22.
- Bartstra, G.-J., 1978. The age of the djetis beds in east and central Java. *Antiquity* 52, 56.
- Berghuis, H.W.K., Troelstra, S.R., Zaim, Y., 2019. Plio-pleistocene foraminiferal biostratigraphy of the eastern Kendeng zone (Java, Indonesia): the marmoy and sumberingin sections. *Palaeogeogr. Palaeoclimatol. Palaeoecol.* 528, 218–231. <https://doi.org/10.1016/j.palaeo.2019.05.008>.
- Bintanja, R., van de Wal, R.S.W., 2008. North American ice-sheet dynamics and the onset of 100,000-year glacial cycles. *Nature* 454, 869–872. <https://doi.org/10.1038/nature07158>.
- Bird, M.I., Taylor, D., Hunt, C., 2005. Palaeoenvironments of insular southeast Asia during the last glacial period: a savanna corridor in sundaland? *Quat. Sci. Rev.* 24, 2228–2242.
- Bull, W.B., 1990. Stream-terrace genesis: implications for soil development. *Geomorphology* 3, 351–367.
- Carthaus, E., 1911. Zur Geologie von Java, insbesondere des Ausgrabungsgebietes. In: *Selenka und Blanckenhorn Die Pithecanthropusschichten Auf Java Geologische Und Palaontologische Ergebnisse De Trinil-Expedition (1907 Und 1908)*. Verlag Von Wilhelm Engelmann, Leipzig, pp. 1–33.
- Cas, R.A.F., Wright, J.V., 1987. *Volcanic Successions: Ancient and Modern*. Allen and Unwin, London.
- Clements, B., Hall, R., Smyth, H.R., Cottam, M.A., 2009. Thrusting of a volcanic arc: a new structural model for Java. *Petrol. Geosci.* 15, 159–174.
- De Vos, J., 1982. The fauna from Trinil, type locality of *Homo erectus*: a reinterpretation. *Geol. Mijnbouw* 61, 207–211.
- Dean, W.E., Kennett, J.P., Behl, R.J., Nicholson, C., Sorlien, C.C., 2015. Abrupt termination of marine isotope stage 16 (termination VII) at 631.5 ka in Santa Barbara Basin, California. *Paleoceanogr. Paleoclimatol.* 30 (10), 1373–1390.
- Dennell, R., 2009. *The Palaeolithic Settlement of Asia*. Cambridge University Press.
- Dozy, C.M., 1911. Bemerkungen zur Stratigraphie der Sedimente in der Triniler Gegend. In: *Selenka und Blanckenhorn: Die Pithecanthropus-Schichten Auf Java. Geologische Und Palaontologische Ergebnisse Der Trinil-Expedition (1907 Und 1908)*. Verlag Von Wilhelm Engelmann, Leipzig.
- Dubois, 1908. Das geologische alter der Kendeng-oder trinil-fauna. *Tijdschrift van het Koninklijk Nederlandsch Aardrijkskundig Genootschap* 1235–1270.
- Dubois, 1907. Eenige van Nederlandschen kant verkregen uitkomsten met betrekking tot de kennis der Kendeng-fauna (fauna van Trinil). *Tijdschrift van het Koninklijk Nederlandsch Aardrijkskundig Genootschap* 449–458.
- Dubois, 1895. *Pithecanthropus erectus*, betrachtet als eine wirkliche Uebergangsform und als Stammform des Menschen. *Z. Ethnol.* 723–738.
- Dubois, 1894a. *Pithecanthropus erectus*: eine menschenaehnliche Uebergangsform aus Java. *Landesdruckerei Batavia*.
- Dubois, 1894b. *Palaeontologische Onderzoekingen Op Java. Verslag van het Mijnwezen*.
- Dubois, 1893. *Palaeontologische Onderzoekingen Op Java. Verslag van het Mijnwezen*.
- Dunham, R.J., 1962. Classification of Carbonate Rocks According to Depositional Textures, vol. 38, pp. 108–121.
- Duyfjes, J., 1938. Toelichting Bij Blad 110 (Modjokerto), Geologische Kaart Van Java Schaal 1: 100.000. Bandung. Dienst van den Mijnbouw in Nederlandsch-Indie.
- Duyfjes, J., 1936. Zur Geologie und Stratigraphie des Kendenggebietes zwischen Trinil und Soerabaja (Java). *De Ingenieur ned.-Indie* 4, 136–149.
- Elbert, 1908. Ueber das Alter der Kendeng-Schichten mit Pihecanthropus erecus Dubois. *Neues Jahrbuch fur Minera-logie, Geologie und Paleontologie* 648–662.
- Evans, D.L., Quinton, J.N., Tye, A.M., Rodés, A., Davies, J.A.C., Mudd, S.M., Quine, T.A., 2019. Arable soil formation and erosion: a hillslope-based cosmogenic nuclide study in the United Kingdom. *SOIL* 5, 253–263.
- FAO, 2015. *World Reference Base for Soil Resources 2014, International Soil Classification System for Naming Soils and Creating Legends for Soil Maps Update 2015, World Soil Resources Reports*. Food and Agriculture Organization of the United Nations.
- Farani, G.L., Nogueira, M.M., Johnsson, R., Neves, E., 2015. The salt tolerance of the freshwater snail *Melanoides tuberculata* (Mollusca, Gastropoda), a bioinvader gastropod. *Pan Am. J. Aquat. Sci.* 10, 212–221.
- Fauzi, M.R., Ansyori, M.M., Prastiningtyas, D., Intan, M.F.S., Wibowo, U.P., Wulandari, Rahmanendra H., Widianto, H., Simanjuntak, T., 2016. Matar: a forgotten but promising Pleistocene locality in east Java. *Quaternary International, Southeast Asia: human evolution, dispersals and adaptation* 416, 183–192. <https://doi.org/10.1016/j.quaint.2015.12.091>.
- Ferreira, T.O., Nóbrega, G.N., Albuquerque, A.G., Sartor, L.R., Gomes, I.S., Artur, A.G., Otero, X.L., 2015. Pyrite as a proxy for the identification of former coastal lagoons in semi-arid NE Brazil. *Geo Mar. Lett.* 35, 355–366.
- Fisher, R.V., Schmincke, H.-U., 1984. *Pyroclastic Rocks*. Springer Science & Business Media.
- Gibbard, P.L., Lewin, J., 2002. Climate and related controls on interglacial fluvial sedimentation in lowland Britain. *Sediment. Geol.* 151, 187–210.
- for I. Hamilton, W.B., Pertambangan, I.D., Development, U.S.A., 1979. *Tectonics of the Indonesian Region*. U.S. Govt. Print. Off.
- Hampton, B.A., Horton, B.K., 2007. Sheetflow fluvial processes in a rapidly subsiding basin, Altiplano plateau, Bolivia. *Sedimentology* 54, 1121–1148. <https://doi.org/10.1111/j.1365-3091.2007.00875.x>.
- Hartono, U., 1994. *The Petrology and Geochemistry of the Wilis and Lawu Volcanoes, East Java, Indonesia (Phd)*. University of Tasmania.
- Heaney, L.R., 1991. A synopsis of climatic and vegetational change in Southeast Asia. In: *Tropical Forests and Climate*. Springer, pp. 53–61.
- Huffman, O.F., De Vos, J., Berkhout, A.W., Aziz, F., 2010. Provenience reassessment of the 1931–1933 Ngandong *Homo erectus* (Java), confirmation of the bone-bed origin reported by the discoverers. *PaleoAnthropology* 2010, 1–60.
- Indriati, et al., 2011. The Age of the 20 Meter Solo River Terrace, Java, Indonesia and the Survival of *Homo Erectus* in Asia. *PlosOne*.
- Janssen, R., Joordens, J.C., Koutamanis, D.S., Puspaningrum, M.R., de Vos, J., Van Der Lubbe, J.H., Reijmer, J.J., Hampe, O., Vonhof, H.B., 2016. Tooth enamel stable isotopes of Holocene and Pleistocene fossil fauna reveal glacial and interglacial paleoenvironments of hominins in Indonesia. *Quat. Sci. Rev.* 144, 145–154.
- Joordens, J.C., d'Errico, F., Wesselingh, F.P., Munro, S., de Vos, J., Wallinga, J., Ankjærgaard, C., Reimann, T., Wijbrans, J.R., Kuiper, K.F., 2015. *Homo erectus* at Trinil on Java used shells for tool production and engraving. *Nature* 518, 228–231.
- Lavigne, F., Thouret, J.-C., Hadmoko, D.S., Sukatja, C.B., 2007. Lahars in Java: initiations, dynamics, hazard assessment and deposition processes. *Forum Geografi* 21, 17–32.
- Lehmann, H., 1936. *Morphologische studien auf Java*. Engelhorn.
- Louys, J., Roberts, P., 2020. Environmental drivers of megafauna and hominin extinction in Southeast Asia. *Nature* 1–5.
- Lunt, P., 2013. *The Sedimentary Geology of Java*. Indonesian Petroleum Association.
- Maddy, D., Veldkamp, A., Jongmans, A.G., Candy, I., Demir, T., Schoorl, J.M., van der Schriek, T., Stemerding, C., Scaife, R.G., van Gorp, W., 2012. Volcanic disruption and drainage diversion of the palaeo-hudut river, a tributary of the early Pleistocene gediz river, western Turkey. *Geomorphology* 165–166, 62–77. <https://doi.org/10.1016/j.geomorph.2011.12.032>.
- Mayr, E., 1950. Taxonomic categories in fossil hominids. In: *Cold Spring Harbor Symposia on Quantitative Biology*. Cold Spring Harbor Laboratory Press, pp. 109–118.
- Miall, A.D., 2014. *Fluvial Depositional Systems*. Springer, Berlin.
- Miall, A.D., 1996. *The Geology of Fluvial Sediments*. Springer, Berlin.
- Miall, A.D., 1977. *Fluvial Sedimentology*: Hist. Rev. 1–47.
- Moormann, van Bremen, 1978. *Rice: Soil, Water, Land*. International rice research institute.
- Oppenorth, 1932. Een Nieuwe Fossiele Mensch Van Java. *Tijdschrift van het Koninklijk Nederlandsch Aardrijkskundig Genootschap*, pp. 704–708.
- Pannekoek, A.J., 1949. *Outline of the Geomorphology of Java*.
- Paredes, J.M., Foix, N., Piñol, F.C., Nillni, A., Allard, J.O., Marquillas, R.A., 2007. Volcanic and climatic controls on fluvial style in a high-energy system: the lower cretaceous matasiete formation, golfo san jorge basin, Argentina. *Sediment. Geol.* 202, 96–123.
- Polhaupessy, A.A., 1990. *Late Cenozoic Palynological Studies on Java (PhD Thesis)*. University of Hull.
- Pons, L.J., Van Breemen, N., Driessen, P.M., 1982. Physiography of coastal sediments and development of potential soil acidity. *Acid Sulfate Weathering* 10, 1–18.
- Pringgoprawiro and Baharuddin, 1979. *Biostratigrafi foraminifera planktonic dan bidang-bidang pengenal kaenozoikum-akhirdari sumur-sumur tobo, cepu, jawa timur*. In: *Proceedings PIT VIII Ikatan Ahli Geologi Indonesia, Jakarta*, pp. 21–31.
- Puspaningrum, M.R., van den Bergh, G.D., Chivas, A.R., Setiabudi, E., Kurniawan, I., 2020. Isotopic reconstruction of proboscidean habitats and diets on Java since the early Pleistocene: implications for adaptation and extinction. *Quat. Sci. Rev.* 228, 106007. <https://doi.org/10.1016/j.quascirev.2019.106007>.
- Rizal, Y., Westaway, K.E., Zaim, Y., van den Bergh, G.D., Bettis, E.A., Morwood, M.J., Huffman, O.F., Grün, R., Joannes-Boyau, R., Bailey, R.M., Sidarto, Westaway M.C.,

- Kurniawan, I., Moore, M.W., Storey, M., Aziz, F., Suminto, Zhao J., Aswan, Sipola M.E., Larick, R., Zonneveld, J.-P., Scott, R., Putt, S., Ciochon, R.L., 2020. Last appearance of *Homo erectus* at Ngandong, Java, 117,000–108,000 years ago. *Nature* 577, 381–385. <https://doi.org/10.1038/s41586-019-1863-2>.
- Roychoudhury, A.N., Kostka, J.E., Van Cappellen, P., 2003. Pyritization: a palaeoenvironmental and redox proxy reevaluated. *Estuarine, Coastal and Shelf Science* 57, 1183–1193.
- Sáez, A., Valero-Garcés, B.L., Moreno, A., Bao, R., Pueyo, J.J., González-Sampériz, P., Giralt, S., Taberner, C., Herrera, C., Gibert, R.O., 2007. Lacustrine sedimentation in active volcanic settings: the Late Quaternary depositional evolution of Lake Chungará (northern Chile). *Sedimentology* 54, 1191–1222. <https://doi.org/10.1111/j.1365-3091.2007.00878.x>.
- Satyana, A.H., Erwanto, E., Prasetyadi, C., 2004. Rembang-madura-kangean-sakala (RMKS) fault zone, East Java basin: the origin and nature of A geologic border. In: *Proc. IAGI, 33rd., Ann. Conv. And Exh., Bandung*.
- Scott, K.M., 1988. Origins, Behavior, and Sedimentology of Lahars and Lahar-Runout Flows in the Toutle-Cowlitz River System.
- Scott, K.M., Macías, J.L., Naranjo, J.A., Rodríguez, S., McGeehin, J.P., 2001. Catastrophic Debris Flows Transformed from Landslides in Volcanic Terrains: Mobility, Hazard Assessment, and Mitigation Strategies. U.S. Department of the Interior, U.S. Geological Survey.
- Selenka, L., Blanckenhorn, M.L.P., 1911. Die Pithecanthropus-Schichten auf Java: Geologische und paläontologische Ergebnisse der Trinil-Expedition (1907 und 1908), ausgeführt mit Unterstützung der Akademischen Jubiläumstiftung der Stadt Berlin und der Königlich bayerischen Akademi der Wissenschaften. W. Engelmann.
- Sémah, A.-M., Sémah, F., 2012. The rain forest in Java through the Quaternary and its relationships with humans (adaptation, exploitation and impact on the forest). *Quat. Int.* 249, 120–128. <https://doi.org/10.1016/j.quaint.2011.06.013>.
- Sémah, A.-M., Sémah, F., Djubiantono, T., Brasseur, B., 2010. Landscapes and hominids' environments: changes between the lower and the early middle Pleistocene in Java (Indonesia). *Quat. Int.* 223, 451.
- Sipola, M.E., 2018. Formation of the Ngandong Paleoanthropological Site and Solo River Terrace Sequence, Central Java, Indonesia.
- Smyth, H.R., Hall, R., Nichols, G.J., 2008. Cenozoic volcanic arc history of East Java, Indonesia: the stratigraphic record of eruptions on an active continental margin. *Spec. Pap. Geol. Soc. Am.* 436, 199.
- Soeradi, et al., 1985. Geology and stratigraphy of the Trinil area. In: *Quaternary Geology of the Hominid Fossil Bearing Formations in Java*. Geological Research and Development Centre Special Publication, Bandung, pp. 49–53.
- Soeria-Atmadja, R., Maury, R.C., Bellon, H., Pringgoprawiro, H., Polve, M., Priadi, B., 1994. Tertiary magmatic belts in Java. *J. Southeast Asian Earth Sci.* 9, 13–27.
- Sondaar, P.Y., 1984. Faunal evolution and the mammalian bio stratigraphy of Java. The early evolution of man with special emphasis on southeast Asia and africa. *Cour. Forsch. Inst. Senckenberg, Frankfurt am Main* 69, 219–235.
- Ter Haar, C., 1934. Het Ngandong Terras, Rapport over Ontdekking, Uitgraving en Geologische Ligging er van uitgebracht [The Ngandong Terrace, Report on the Discovery, Excavation and Geological relationships]. Geological Library (prepared for signature on 27 July).
- Tucker, M.E., 1985. Shallow-marine carbonate facies and facies models. Geological Society, London, Special Publications 18, 147–169.
- Vallance, J.W., 2005. Volcanic debris flows. In: *Debris-Flow Hazards and Related Phenomena*. Springer, pp. 247–274.
- van Bemmelen, R.W., 1949. The Geology of Indonesia. 1, A. General Geology of Indonesia and Adjacent Archipelagoes. US Government Printing Office.
- Van Benthem Jutting, 1937. Non marine Mollusca from fossil horizons in Java with special reference to the Trinil fauna. *Zoologische Mededelingen* 20, 83–180.
- Van den Bergh, G.D., de Vos, J., Sondaar, P.Y., 2001. The Late Quaternary palaeogeography of mammal evolution in the Indonesian Archipelago. *Palaeogeogr. Palaeoclimatol. Palaeoecol.* 171, 385–408.
- Van den Bergh, G.D., de Vos, J., Sondaar, P.Y., Aziz, F., 1996. Pleistocene zoogeographic evolution of Java (Indonesia) and glacio-eustatic sea level fluctuations: a background for the presence of Homo. *Bulletin of the Indo-Pacific Prehistory Association* 14, 7–21.
- Van der Geer, A.A., 2019. Selenka and Blanckenhorn die pithecanthropusschichten auf Java geologische und palaontologische ergebnisse de trinil-expedition (1907 und 1908) verlag von wilhelm engelmann, leipzig. *PeerJ* 7, e6894.
- Van der Kaars, S., Wang, X., Kershaw, P., Guichard, F., Setiabudi, D.A., 2000. A Late Quaternary palaeoecological record from the Banda Sea, Indonesia: patterns of vegetation, climate and biomass burning in Indonesia and northern Australia. *Palaeogeogr. Palaeoclimatol. Palaeoecol.* 155, 135–153.
- Van Es, L.J.C., 1931. The Age of Pithecanthropus. Springer.
- Van Gorsel, J.T., Troelstra, S.R., 1981. Late Neogene planktonic foraminiferal biostratigraphy and climatostratigraphy of the Solo River section (Java, Indonesia). *Mar. Micropaleontol.* 6, 183–209. [https://doi.org/10.1016/0377-8398\(81\)90005-0](https://doi.org/10.1016/0377-8398(81)90005-0).
- Veldkamp, A., Schoorl, J.M., Wijbrans, J.R., Claessens, L., 2012. Mount Kenya volcanic activity and the Late Cenozoic landscape reorganisation in the upper Tana fluvial system. *Geomorphology* 145, 19–31.
- Veldkamp, A., van Dijke, J.J., 2000. Simulating internal and external controls on fluvial terrace stratigraphy: a qualitative comparison with the Maas record. *Geomorphology* 33, 225–236. [https://doi.org/10.1016/S0169-555X\(99\)00125-7](https://doi.org/10.1016/S0169-555X(99)00125-7).
- Volz, W., 1907. Das geologische Alter der Pithecanthropus-Schichten bei Trinil, Ost-Java. *Schweizerbart*.
- Von Koenigswald, G.H.R., 1935. Die saugtierfaunen javas. *Proc. Kon. Akad.v. Wetensch, Amsterdam* 38, 188–198.
- Von Koenigswald, G.H.R., 1934. Zur Stratigraphie des Javanischen Pleistocan. *De Ingenieur in Nederlands-Indie* 1, 185–201.
- Weaver, C.E., 1989. Clays, Muds, and Shales. Elsevier.
- Wentworth, C.K., 1922. A scale of grade and class terms for clastic sediments. *J. Geol.* 30, 377–392.
- Wright, V.P., 1984. Peritidal carbonate facies models: a review. *Geol. J.* 19, 309–325.
- Zaim, Y., 2010. Geological evidence for the earliest appearance of hominins in Indonesia. In: *Out of Africa I*. Springer, pp. 97–110.